Variability of Summer Rainfall over Southwestern Madagascar

Tsinampoizina Marie Sophie Randriamahefasoa

Department of Oceanography
University of Cape Town

Dissertation presented for the degree of Master of Science at the University of Cape Town

February 26, 2013

Declaration

I declare that this thesis is my own work and has not been submitted in any form for another degree or diploma at any university or other institute of tertiary education. Information derived from the published and unpublished work of others has been acknowledged in the text and a list of references is given.

Signed by candidate

T.M.S. Randriamahefasoa

February 26, 2013

Date

To my country Madagascar,

Abstract

This study investigates the interannual variability of the frequency of wet days during the rainy season over southwestern Madagascar, and its associated regional and global circulation patterns. The number of wet days was counted for each summer season (December to March) of the period 1971 to 2000 at four rainfall stations in southwestern Madagascar. For each station, the frequency of wet days was correlated with ENSO indices, SIOD index, SST, 850 hPa geopotential height, zonal and meridional winds at the surface. Composite anomalies of moisture flux and moisture flux convergence at 850 hPa, 500 hPa omega and velocity potential at .995 sigma level, using NCEP/NCAR reanalysis data, associated with El Niño events, La Niña events that occurred during the period of study were examined. Also, circulation anomalies during neutral years having anomalously high frequency of wet days or anomalously low frequency of wet days were analysed separately.

It was found that the number of wet days rarely exceeds half of the total days in summer for each station. Inverse relationship between the equatorial Pacific SST anomalies and the frequency of wet days anomalies was identified. Statistics showed that years characterised by high frequency of wet days often occur with La Niña seasons whereas years having low frequency of wet days tend to occur with El Niño seasons. A strong relationship between the southern Indian Ocean SST and the frequency of wet days was found at Ranohira (45.3°E, 22.5°S) and Toliara (43.72°E, 23.38°S). Increased number of wet days over southwestern Madagascar is associated with low atmospheric pressure over the southern Mozambique Channel. Neutral years having anomalously high (low) frequency of wet days are marked by northwesterly (southeasterly) moisture flux anomalies at 850 hPa over southwestern Madagascar.

Acknowledgements

I thank God for giving me strength during my study. I would like to thank my supervisor Professor Chris Reason for his guidance on this study and for his great support when I was planning to carry on my study in Oceanography. I am grateful to the Western Indian Ocean - Regional Initiative for Marine Science Education (WIO-RISE) for funding my Master's study in Ocean and Climate Dynamics.

I would like to thank the Meteorological Services of Antananarivo, Madagascar and Dr. Nirivololona Raholijao for providing the rainfall data used in this study. I also thank the following online services: The Koninklijk Nederlands Meteorologisch Instituut (KNMI) Climate Explorer (`http://climexp.knmi.nl`), NOAA/ESRL Physical Sciences Division, Boulder Colorado (`http://www.esrl.noaa.gov/psd/`)

I wish to thank my husband Fortunat Rajaona for his assistance in programming with MATLAB and his moral support.

Contents

List of Figures

List of Tables

Nomenclature

ENSO El Niño Southern Oscillation

ITCZ Intertropical Convergence Zone

SDI Subtropical Dipole Index

SIOD Subtropical Indian Ocean Dipole

SOI Southern Oscillation Index

SST Sea Surface Temperature

TC Tropical Cyclone

Chapter 1

Introduction

This chapter introduces Madagascar, the variations of its landforms and the main wind circulation over the country. The patterns of summer rainfall in different regions are discussed. Interests and objectives of this study end this chapter.

1.1 Madagascar location and topography

The island of Madagascar is located in the southwestern Indian Ocean and to the southeast of the African continent, between the latitudes 12°S and 26°S and the longitudes 43°E and 51°E (Figure 1.1). It is separated from mainland Africa by the Mozambique Channel. Madagascar can be considered as a small subcontinent because of its insularity and its size (592 800 km^2) which is about half the size of South Africa. It is the fourth largest island in the world. Also, the island has a remarkable structure of landforms and various climatic conditions.

Madagascar has a complex topography but generally it is dominated from north to south by plateaus of altitude between 800 m and 1600 m, which occupy two third of the land surface. Through its length, Madagascar shows ranges of mountains from the massif of Tsaratanana located in the north which has the highest peak of the island (2886 m at Maromokotro) to the massif of Ivakoany (1900 m of altitude) in the south. Ankaratra and Andringitra massifs are situated in centre. These mountain ridges constitute a barrier between the eastern and the western part of Madagascar.

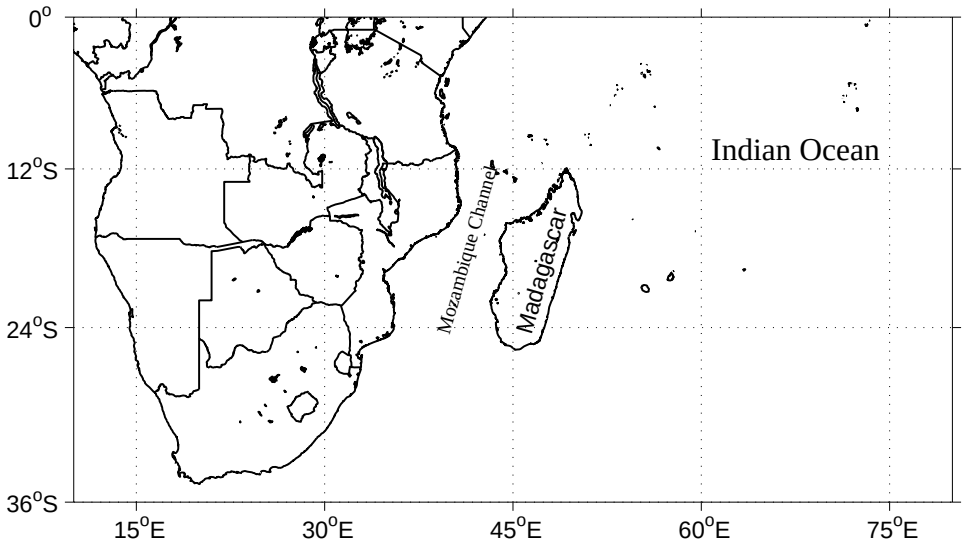

Figure 1.1: Madagascar location (between the latitudes 12°S and 26°S and the longitudes 43°E and 51°E)

The central highlands is bordered in the east by the cliff of Angavo and the Betsimisaraka escarpment (Figure 1.2). A narrow coastal strip separates these steep slopes from the Indian Ocean. In contrast, the descent to the west from the central highlands is less abrupt, it is constituted by series of hills and plains. These features favour a windward slope in the eastern part and a leeward in the western part for the southeasterly trade wind.

The area of study is southwestern Madagascar (Figure 1.2). It is bordered in the southeast by the massif of Ivakoany and the mountain ranges of Anosy and Vohimena nearby Taolagnaro station (Figure 2.1). From this station to the western coast, there are successively the plateau of Ihorombe, the massif of Isalo where Ranohira station is located (Figure 2.1) and the massifs of Analavelona and Mikobaka. The extreme south is dominated by the plateaus of Mahafaly and Karimbola.

[1]Map drawn with MATLAB (2012a) and READHGT toolbox with STRM land elevation data found at `http://dds.cr.usgs.gov/srtm/version2_1`

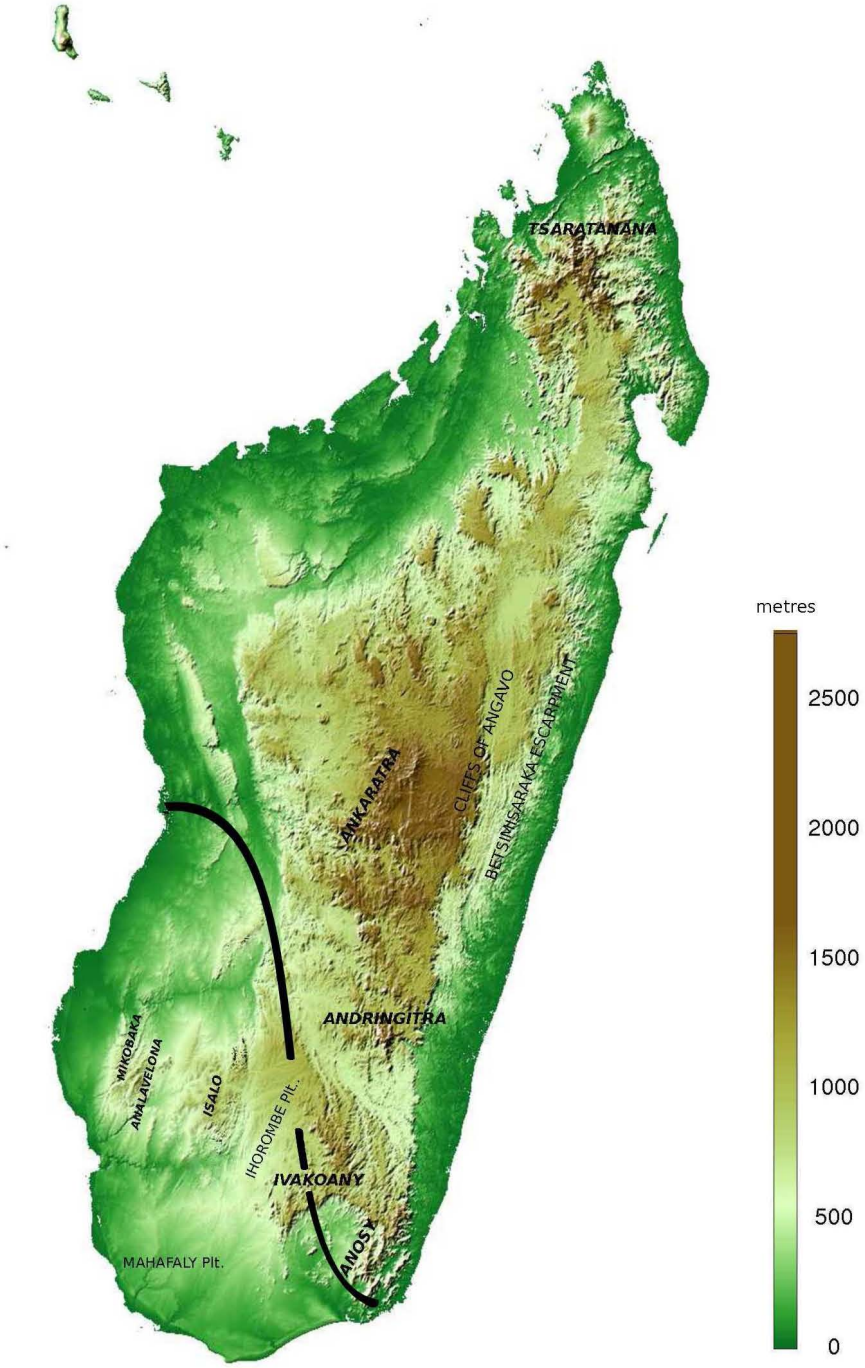

Figure 1.2: Topography of Madagascar[1]. The region of study is the southwestern part (west of the black line): delimited in the north by the latitude of Morondava (20° S), in the west by the Mozambique Channel, in the east by the massifs of Andringitra and Ivakoany.

1.2 Spatial distribution of rainfall over Madagascar

Previous research (Donque, 1975; Pelleray, 1954; Williams, 1990) found that different wind regimes and the structure of topography are part of the factors that influence climatic variability on the island of Madagascar. The southeasterly trade wind and the northwesterly monsoon with their interaction play an important role in the distribution of rainfall over the country. In addition, during the summer Madagascar, is affected by tropical cyclones (TC) originating often from western tropical Indian Ocean or rarely from the Mozambique Channel.

The prevailing southeasterly trade wind originates from the south Indian Ocean. It reaches the eastern coast of Madagascar bringing moisture from the Indian Ocean. Its circulation is disrupted by the land elevation and enhanced rainfall may result from the landforms effect. Consequently, the eastern region is rainy throughout the year with a short decrease of the rain only in August-September. This leads to high annual rainfall, above 2000 mm in many stations (e.g 3370 mm at Toamasina (18°09′S, 49°25′E), 2340 mm at Antalaha (14°53′S, 50°17′E)[2]). The variation of rainfall in eastern Madagascar depends mainly on the distance from the coast and the altitude (Pelleray, 1954). In addition, TCs formed in the tropical western Indian Ocean may also bring strong intensity of rainfall to the eastern part of Madagascar. Most of the TCs from the north east of Madagascar reach the island between Toamasina (18°09′S, 49°25′E) and Vohemar (13°35′S, 50°E), both of them are located on the eastern coast.

The northwesterly monsoon blows over the nothwestern region of Madagascar during summer, causing intense rainfall. Although the region experiences drier winter, rainfall during the summer is more intense than it is in the eastern part of Madagascar (Williams (1990) noticed that mean monthly rainfall for summer is between 390 mm and 470 mm in the northwest whilst only between 280 mm and 340 mm in the east). TCs from the tropical western Indian Ocean moving westward also affect the eastern part.

The confluence of the monsoon and the trade winds which is the Inter Tropical Convergence Zone (ITCZ) crosses Madagascar during January and February bringing convective rainfall; the ITCZ moves southward and reaches as far as 17–20°S near the longitudes 44–45°E before retreating northward (Donque, 1975; Jury and Pathack, 1991). The central highlands

[2]Mean annual rainfall amount of the period 1971–2000

receive moderate amount of summer rainfall, peaking in January–February, which are mostly caused by convective clouds. The centre experiences less dry winter than the northwestern area. Due to the presence of central mountain ridges such as Andringitra, Ankaratra and Ivakoany (Figure 1.2), the prevailing trade wind moving westward loses much of its humidity before reaching the west coast.

Southwestern Madagascar is the driest part of the island, it receives the lowest annual rainfall (between 300 mm and 1000 mm). The region is less affected by seasonal monsoon and the ITCZ. The displacement of the ITCZ during summer is limited north of 20°S. Despite many tropical cyclones having impacts on many regions of Madagascar, few of them affect southwestern Madagascar. According to the statistics done by Poisson (1936) and Pelleray (1954), 20 tropical cyclones affected southern Madagascar during the period of 1848 to 1952, i.e for about more than one century. Only few of them are known of strong intensity and brought extreme rainfall over southern Madagascar. The summer rainfall in this region depends mostly on the strength of the trade wind (Williams, 1990). The precipitation caused by the southeasterly trade wind is affected by the topography and the location: precipitation rate decreases westward, and it increases with the altitude.

In summary, the winds regime blowing over different parts of Madagascar and landforms cause significant variations in the spatial distribution of rainfall over Madagascar as well as the TCs.

1.3 Objectives of the study

Very little research has been undertaken on the climate variability of Madagascar. Jury et al. (1995) studied the rainfall variability of Madagascar at interannual scale with emphasis on the central region. Nassor and Jury (1997, 1998) studied the intra-seasonal climate variability of the northwestern region. This study aims to add to this research by examining interannual rainfall variability in southwestern Madagascar (Figure 1.2).

Like many regions of the island, population activity in southwestern Madagascar is based on agriculture. Substantial rainfall plays an important role for crop production such as rice and maize. Droughts or late rainfall have severe consequences. Crop failure may result directly into famine for rural population in southwestern Madagascar.

This study investigates the distribution of *the number of wet days* during the summer season in southwestern Madagascar. The research aims to advance understanding of the variations of the frequency of wet days by answering the following questions:

1. How does the number of wet days vary from one year to the next? and
2. What are the regional and global circulation patterns that could be associated with the frequency of wet days variability in southwestern Madagascar during the period of study?

In order to answer the research questions, Chapter 2 focuses on rainfall data, climate indices, atmospheric and oceanic data used. The method used for each data set are also discussed in this chapter. The first basic results are described in Chapter 3: the number of wet days and its variation for each station studied, the correlation between the frequency of wet days and climate indices followed by correlation maps with various fields such as SST, 850 hPa geopotential height and winds. Chapter 4 focuses on the regional circulation anomalies that could be associated with anomalous wet and dry years that occurred in southwestern Madagascar. In Chapter 5, the summary of the findings concludes the study.

Chapter 2

Data and methodology

2.1 Rainfall data

Rainfall data from the Meteorological Services of Antananarivo, Madagascar were used for this study. Data were collected by raingauges and range from January 1971 to December 2000. For the southwestern region, daily rainfall data were available for four stations (Figure 2.1): Morondava (20°17′S, 44°18′E) on the west coast and northern limit of the area of study; Toliara also known as Tuléar (23°22′S, 43°39′E) situated on the west coast; Ranohira (22°33′S, 45°24′E) located inland at 825 m altitude and Taolagnaro also known as Fort-Dauphin (25°1′S, 46°59′E) on the east coast surrounded by the mountain range of Anosy.

This study is based on the number of wet days at these four stations. A wet day is a day with rainfall more than 1 mm; a heavy rain day is a wet day with rainfall more than 30 mm (British Rainfall Organisation). The wet days and heavy rain days of each month of the years of the period 1971–2000 were calculated.

The monthly climatology of the frequency of wet days are calculated for the period of study. The mean frequency of wet days for each month over the period of 30 years is computed. For example

$$\overline{f_{\mathsf{Jan}}} = \frac{f_{\mathsf{Jan}}(1971) + f_{\mathsf{Jan}}(1972) + \ldots + f_{\mathsf{Jan}}(2000)}{30}.$$

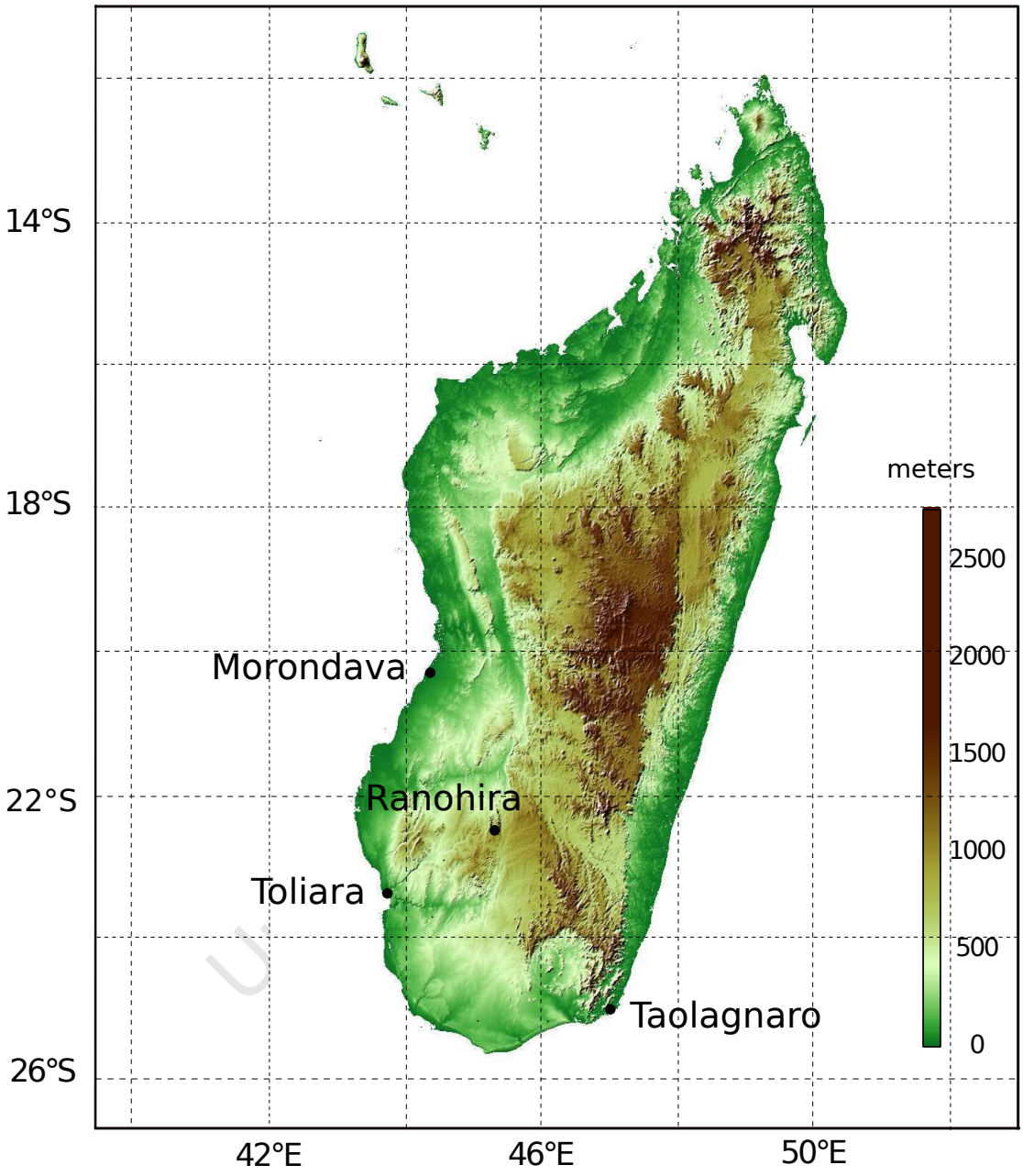

Figure 2.1: Daily rainfall station: Morondava (20°17′S, 44°18′E), Toliara (23°22′S, 43°39′E), Ranohira (22°33′S, 45°24′E), Taolagnaro (25°1′S, 46°59′E).

The time series of the frequency of wet days (for Dec–Mar) x_i, such that year i varies from 1971 to 2000, is transformed into series of standardised anomalies of the frequency of wet days z_i. This technique, as explained by Wilks (2005) is used to measure the distance of each data value from the mean $\overline{x}$ of all the data in standard deviation (σ_x) units.

$$z_i = \frac{x_i - \overline{x}}{\sigma_x} \tag{2.1}$$

Rainy seasons with high frequency of wet days are defined as the wettest seasons and rainy seasons with low frequency of wet days are defined as the driest seasons. Wettest (driest) rainy seasons are selected when their standardised anomaly of the frequency of wet days is greater than 1 (less than -1).

2.2 Correlation of the frequency of wet days with climate indices: ENSO indices, SOI, SDI.

El Niño Southern Oscillation (ENSO) is the oceanic phenomenon El Niño associated with the atmospheric phenomenon Southern Oscillation. El Niño is the anomalous warming of SST in the central and eastern equatorial Pacific Ocean, whilst the Southern Oscillation is the oscillation between sea level pressure in the central eastern and the western Pacific. A warm (cold) phase of ENSO called El Niño (La Niña) consists of extreme warm (extreme cold) SST in the central and eastern equatorial Pacific Ocean due to weakening (strengthening) of the easterly trade winds.

To measure the state of El Niño, four indices are defined by the standardised three months average of SST anomaly in four different regions of the equatorial Pacific Ocean: Niño1+2 between 10°S to the Equator and 90°W to 80°W, Niño3 between 5°S to 5°N and 150°W to 90°W, Niño3.4 between 5°S to 5°N and 170°W to 120°W, Niño4 between 5°S to 5°N and 160°E to 150°W. The state of Southern Oscillation is measured by the Southern Oscillation Index namely SOI, obtained from the standardised differences between the standardised monthly sea level pressure anomalies at Tahiti (in the central Pacific Ocean) and Darwin (in Northern Australia).

The influence of El Niño and the Southern Oscillation on rainfall patterns over Africa has been extensively studied (Nicholson and Kim, 1997; Ropelwski, 1987). ENSO phenomenon

Year \ Rain (mm)	Morondava		Ranohira		Taolagnaro		Toliara	
	≥ 1	≥ 30	≥ 1	≥ 30	≥ 1	≥ 30	≥ 1	≥ 30
1971–72	32	4	57	14	50	8	28	3
1972–73	43	9	42	9	39	6	6	0
1973–74	43	12	54	8	52	4	20	4
1974–75	34	7	55	11	54	7	21	3
1975–76	40	4	45	2	35	1	20	4
1976–77	39	11	51	7	54	6	20	4
1977–78	33	2	38	3	38	5	19	3
1978–79	33	6	42	9	42	5	18	1
1979–80	20	3	41	4	55	3	8	0
1980–81	33	6	55	4	36	6	23	4
1981–82	46	14	64	18	55	9	26	6
1982–83	35	5	38	4	25	1	10	1
1983–84	42	11	62	12	62	8	19	2
1984–85	36	3	48	2	42	5	12	3
1985–86	33	5	46	4	37	3	15	2
1986–87	29	4	55	5	41	3	12	2
1987–88	35	8	38	4	29	3	20	4
1988–89	34	5	50	5	51	10	18	4
1989–90	30	7	55	6	51	7	16	1
1990–91	32	9	42	3	27	1	18	0
1991–92	26	6	41	3	43	4	7	0
1992–93	38	9	60	5	41	6	23	0
1993–94	42	11	56	8	61	10	17	1
1994–95	25	8	42	3	46	5	18	4
1995–96	44	13	45	4	51	6	26	4
1996–97	35	5	51	5	40	7	24	2
1997–98	38	6	47	7	45	11	13	2
1998–99	42	6	62	9	60	10	30	8
1999–00	36	9	48	4	37	3	25	1

Table 2.1: Frequency of wet days (rainfall ≥ 1 mm) and heavy rainfall (rainfall ≥ 30 mm) days for Dec–Mar at the four stations.

affects precipitation over Africa for instance increased rainfall in equatorial eastern Africa and decreased rainfall in southeastern Africa regions (Ropelwski, 1987). These tendencies, during the southern summer, suggest that the convective zone over southwest Indian Ocean and adjacent land is displaced equatorward during El Niño (Philander, 1990).

Recently discovered in the Indian Ocean, a positive phase of Subtropical Indian Ocean Dipole (SIOD) consists of a warm SST anomaly in the subtropical southwestern Indian Ocean (south of Madagascar) and a cold SST anomaly in the subtropical southeastern Indian Ocean (off Australia) during austral summer, the negative phase being the opposite pattern. The SST anomaly is caused by an increase or a decrease in evaporation associated with the strength of the winds along the eastern edge of the subtropical high in south Indian Ocean. SIOD involves change in the south Indian Ocean anticyclone: The positive phase of SIOD is associated with southward displacement and strengthening of the subtropical high (Behera and Yamagata, 2001). The state of SIOD is measured by the Subtropical Dipole Index (SDI), obtained from the difference between SST anomaly in the western part of southern Indian Ocean, 37°S to 27°S, 55°E to 65°E and the SST anomaly in its eastern part 28°S to 18°, 90°E to 100°E (Behera and Yamagata, 2001). It was found that SIOD affects austral summer rainfall variability over many regions in south central Africa (Behera and Yamagata, 2001) and summer rainfall variability in southeastern Africa (Reason, 2001).

Both ENSO and SIOD have significant impacts on the trajectories of tropical cyclones in southwest Indian Ocean (Ash and Matyas, 2012).

To detect any ENSO and Indian Ocean SST relationship with summer rainfall over south-western Madagascar, correlation of the frequency of wet days with Niño1+2, Niño3, Niño3.4, Niño4, SOI and SDI were calculated using the following method: Time series of average Dec–Mar of each climate index is correlated with time series of the frequency of wet days in summer for the period 1971–2000. The correlations were computed directly from the KNMI Climate Explorer website[1] using ERSST V3b[2] for Niño indices and SDI, and using NCEP data obtained from CPC[3] for the SOI.

[1]The Koninklijk Nederlands Meteorologisch Instituut (KNMI) Climate Explorer at `http://climexp.knmi.nl`

[2]Extended Reconstructed Sea Surface Temperature (Smith et al., 2008; Xue, Smith, and Reynolds, 2003)

[3]`http://www.cpc.ncep.noaa.gov/data/indices/`

2.3 Spatial correlations of the frequency of wet days with SST, 850 hPa geopotential height and wind fields

To identify any relationship between summer rainfall over southwestern Madagascar and regional and large scale circulation patterns, spatial correlation between the frequency of wet days and global SST during the summer season is plotted directly from the Climate Explorer website. The method used for spatial correlation is similar to that used for the correlation between the frequency of wet days in summer (Dec–Mar) and climate indices (averaging Dec–Mar for the monthly data of the field). Monthly ERSST V3b data were used for the correlation.

Spatial correlations of the frequency of wet days with other fields such as 850 hPa geopotential height over the southern hemisphere, zonal and meridional winds at the surface between the Equator to 40°S and 0° to 100°E are also plotted directly from the Climate Explorer website. Available geopotential height and winds data from NCEP/NCAR reanalysis were used for that purpose.

2.4 Composite analyses

To investigate any regional circulation pattern that could be associated with the frequency of wet days over southwestern Madagascar, composite analyses of extreme wet and dry seasons i.e, seasons with high and reduced number of wet days respectively, were examined. Moisture flux and moisture flux convergence at 850 hPa pressure level (typically just above the boundary layer), omega (vertical velocity) at 500 hPa, velocity potential at .995 sigma level[4] are the atmospheric variables used in the analysis. The climatology of each atmospheric variable for December to March of the period 1971 to 2000, and the composite seasonal anomalies were plotted between 40°S to the Equator and 0° to 100°E. Circulation anomalies during El Niño seasons (summer seasons during which El Niño occurred) and La Niña seasons (summer seasons during which La Niña occurred) of the period 1971 to

[4]The sigma level at a given point is the ratio of the pressure at this point and the surface pressure below it. Thus the .995 sigma level corresponds to points where the pressure is 0.995 times the surface pressure.

2000 were examined. Particular El Niño seasons, La Niña seasons and neutral (neither El Niño nor La Niña) seasons with anomalously high or low frequency of summer wet days were plotted separately to identify the associated circulation anomaly.

Moisture flux was calculated using specific humidity[5] and wind data from NCEP/NCAR reanalysis. The specific humidity q was taken at 850 hPa pressure level as more than half of the water vapour in the atmosphere is concentrated below this level (Peixoto and Oort, 1992); it was multiplied by the wind vector (u, v) (zonal and meridional winds) at the same level to get the moisture flux (qu, qv). The grid box of specific humidity and winds data has a $2.5° \times 2.5°$ horizontal resolution.

The divergence field d is obtained from the moisture flux using the formula:

$$d = \mathsf{div}(qu, qv) = \vec{\nabla}.(qu, qv) = \frac{\partial(qu)}{\partial x} + \frac{\partial(qv)}{\partial y}$$

where $\frac{\partial}{\partial x}$ and $\frac{\partial}{\partial y}$ are the partial derivatives along the longitude and latitude respectively. The moisture flux convergence corresponds to the negative value of the divergence field. It allows the detection of the source regions and the sink regions of water vapour.

To determine the orientation and the speed of the vertical motion of air (sinking or rising) during anomalously wet and dry seasons, composite anomalies of the vertical velocity (omega) at 500 hPa pressure level were plotted. Finally, composite anomalies of the velocity potential at 0.995 sigma level are plotted directly online from the NOAA/ESRL Physical Sciences Division Website, which is a monthly/seasonal climate composite website. The velocity potential variable would indicate the change of the Walker circulation. The Walker circulation or Walker cell is the zonal (east-west) component of ascending and descending mass of air in the west and in the east respectively, or vice-versa, in the tropics.

The specific humidity, the winds, the omega and the velocity potential data used for these analyses are NCEP/NCAR reanalysis data (Kalnay et al., 1996) provided by the NOAA/OAR/ESRL PSD, Boulder, Colorado, USA, from their Website[6]. The moisture flux and moisture flux divergence were calculated with MATLAB (2012a). The plots of moisture flux, moisture flux divergence and omega were done with MATLAB and the

[5]Specific humidity q is the mass of water vapour m_w contained in a unit mass of moist air (dry air plus water vapour) m_a: $q = \frac{m_w}{m_a}$ (g/kg)

[6]`http://www.esrl.noaa.gov/psd/`

M_MAP toolbox.

Chapter 3

Observations

3.1 Annual cycle of precipitation

The number of wet days for each month for the period 1971–2000 was averaged into a monthly climatology of the frequency of wet days (Figure 3.1). The monthly climatology of rainfall is also plotted in Figure 3.2 to confirm the rainy season. The two types of plots (number of wet days and rainfall amount) give a similar annual cycle. Observation of these figures shows that the rainy season at the three western stations: Morondava, Ranohira and Toliara (Figure 2.1) are similar.

At Morondava station, summer rainfall amount is the highest (Figure 3.2), peaking in January–February, although the station has fewer wet days than Ranohira station in summer (Figure 3.1). Summer rainfall is more intense at this station as it might be affected by the seasonal northwesterly monsoon. The southward displacement of the ITCZ might cause the peak of rainfall in January–February. Because of its latitude, easterly trade winds affect precipitation at Ranohira station (Figure 2.1). The summer is wet and the rain starts earlier (in November) as seen in Figure 3.1. Toliara is the driest in summer as seen from the statistics of the number wet days (Figure 3.1d) and the monthly amount of rainfall (Figure 3.2). Taolagnaro station does not have dry season, but a decrease of precipitation is observed in August–October. This station is more influenced by the trade winds. Rainfall patterns can be affected by the presence of a range of mountains surrounding the region, Figure 2.1. Consequently, the effect of topography produces more rain.

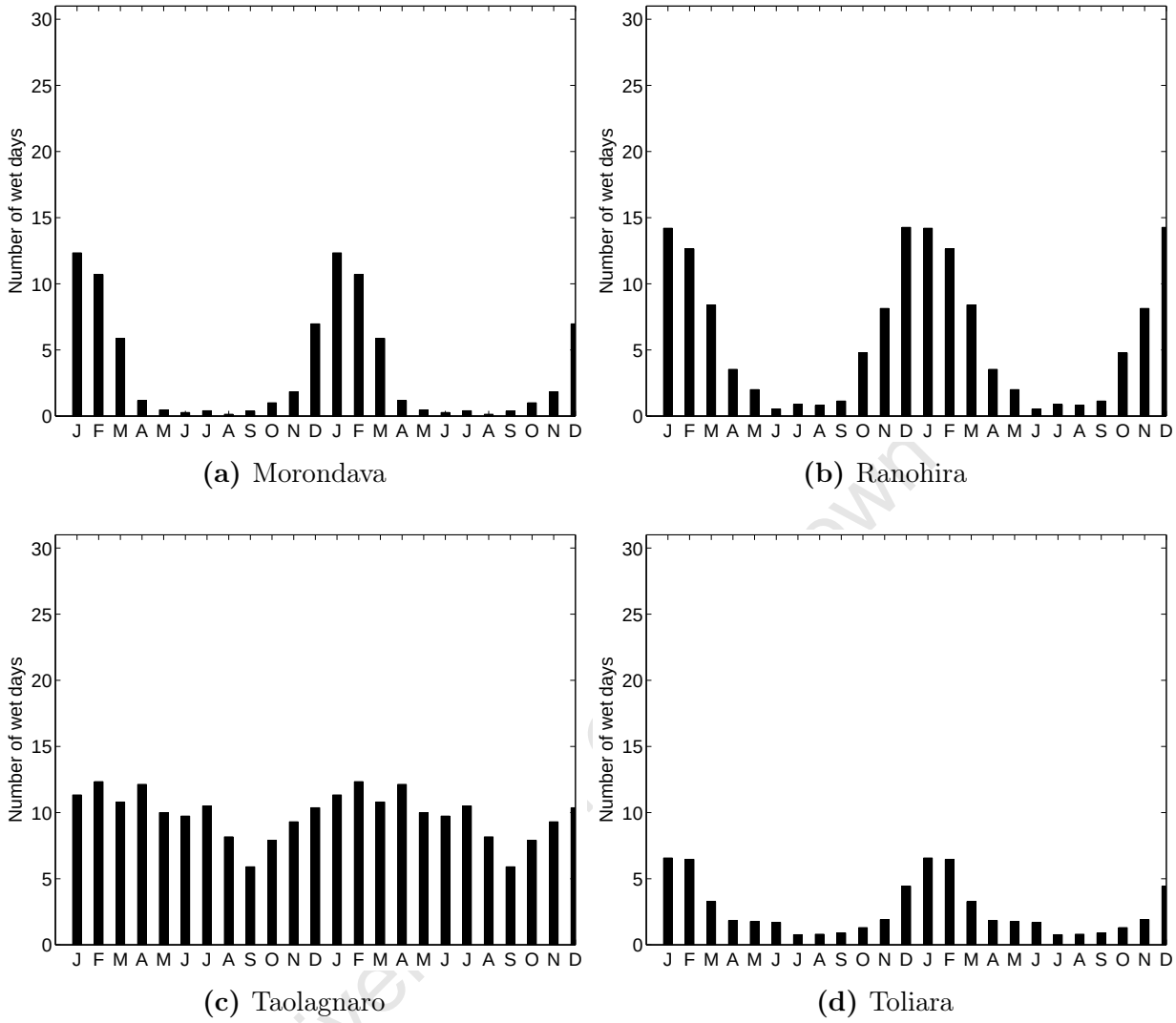

(a) Morondava **(b)** Ranohira

(c) Taolagnaro **(d)** Toliara

Figure 3.1: Monthly climatology of the frequency of wet days of 1971-2000.

According to the graphs of annual cycles based on the number of wet days (Figure 3.1) as well as the graphs of annual cycles based on rainfall amount (Figure 3.2), the rainy season begins in December and ends in March which is the summer season in the southern hemisphere.

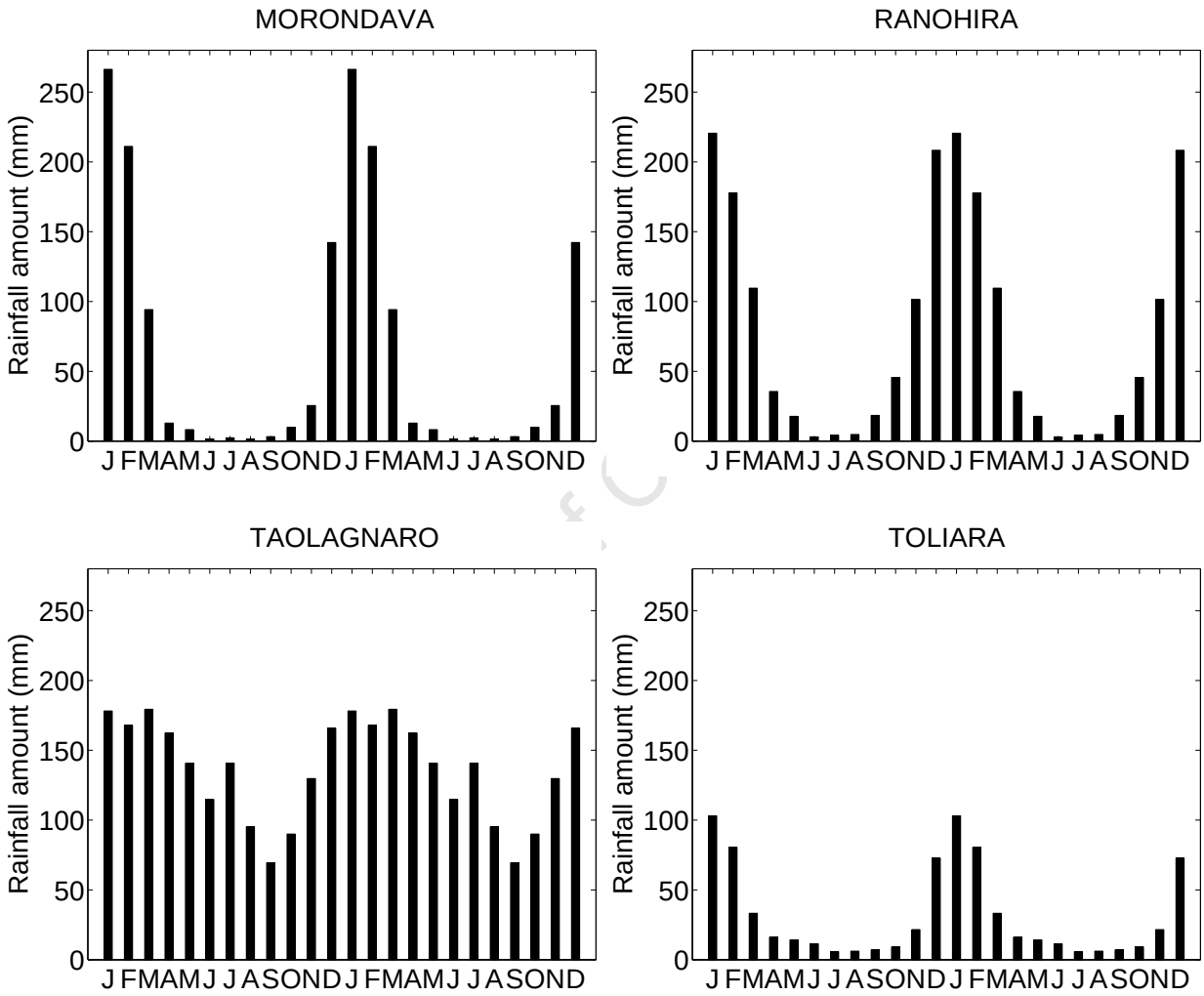

Figure 3.2: Climatology of total monthly rainfall for the period 1960-2000.

3.2 Interannual variability of the frequency of wet days

From December to March, there are 120 days. The statistics of wet days during these four months is shown in Table 2.1. It is observed from Figure 3.3 that southwestern Madagascar receives less precipitation. The number of wet days rarely reaches 60 for the rainy seasons of the period of 1971–2000.

Correlation between the frequency of wet days at Ranohira and Taolagnaro, $r = 0.6367$ with $p = 0.0002$, indicates a strong relationship between the rainfall at the two stations during the rainy season. Significant positive correlation between the frequency of wet days at Ranohira and Toliara stations, $r = 0.5304$ with $p = 0.0031$, suggests that rainfall measured at Ranohira is correlated with rainfall measured at Toliara as these stations are close to each other (Figure 2.1). A direct relationship may exist between the number of wet days at Morondava and Toliara stations, both are located in the western coast, the correlation coefficient is $r = 0.4128$ with $p = 0.0261$. In essence, rainfall over Ranohira station is correlated with rainfall over Toliara station and Taolagnaro station.

Application of Equation (2.1) to the time series of the frequency of wet days for the rainy season was done to normalise the December–March seasonal number of wet days for the four stations studied as illustrated by Figure 3.4. The dotted horizontal lines overlying the bar graphs select the wet period (above 1), years having anomalously high frequency of wet days; and the dry period (below -1), years having anomalously low frequency of wet days. Figure 3.4 shows clearly that there are several years having standard departure of the frequency of wet days more than 1 or less than -1. Selected years show that the wet and dry years vary irregularly for each station as seen in Table 3.1. There exist common wet years or common dry years for some or all of the stations.

Table 3.1 summarizes the wettest and the driest rainy season for each station, according to the method of classification discussed in Section 2.1. Note that years without type are neutral years, neither El Niño nor La Niña. From Figure 3.4 it is clear that other factors, excluding El Niño or La Niña conditions, could affect rainfall over southwestern Madagascar. Some seasons are dry in absence of El Niño, for example 1979–80 was dry at Morondava, Ranohira and Toliara; and some seasons are wet in absence of La Niña, for example 1981–82 was a wet season for the four stations.

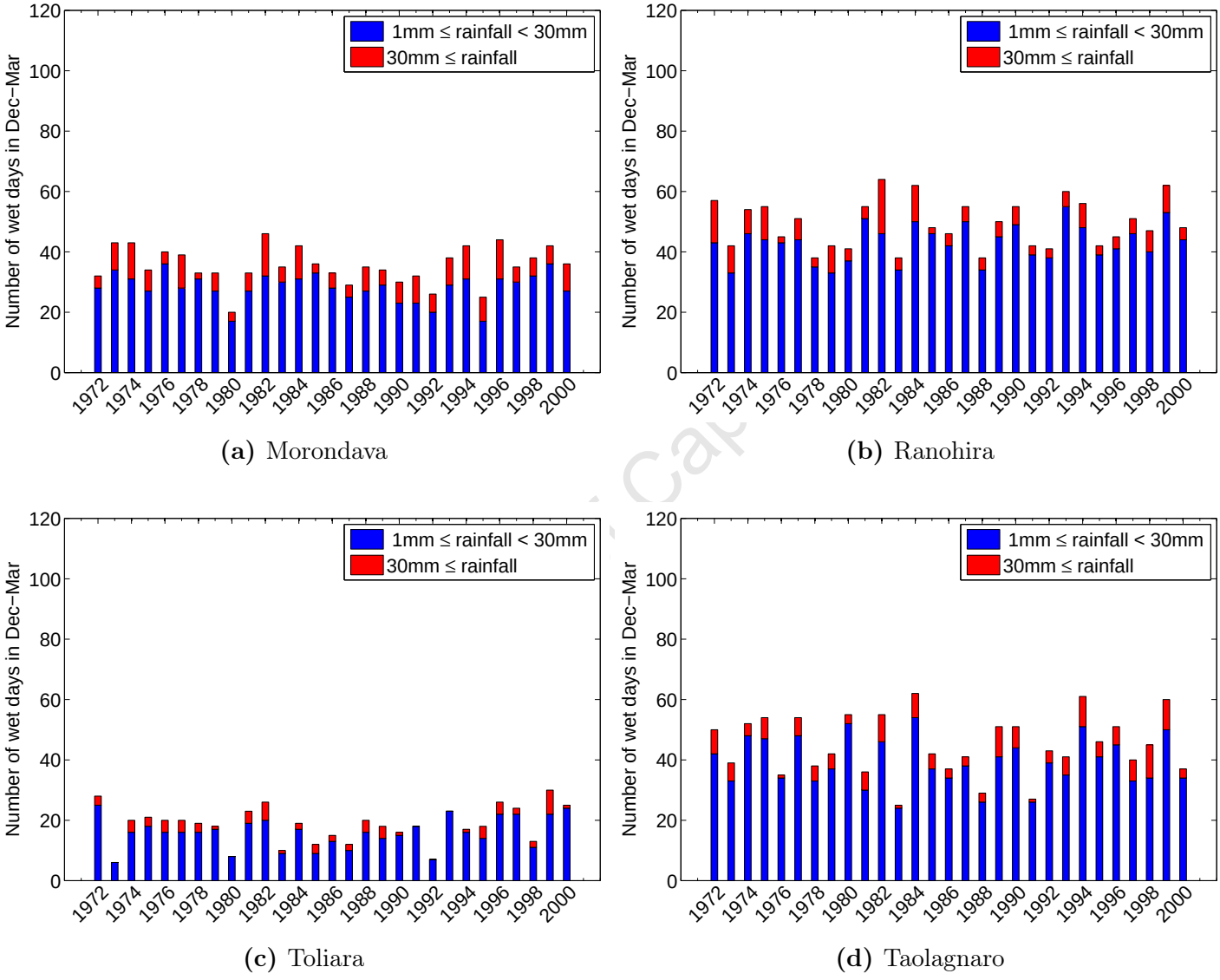

(a) Morondava **(b)** Ranohira

(c) Toliara **(d)** Taolagnaro

Figure 3.3: Frequency of wet days (heavy rainfall days in red) for Dec–Mar of the years 1971–2000.

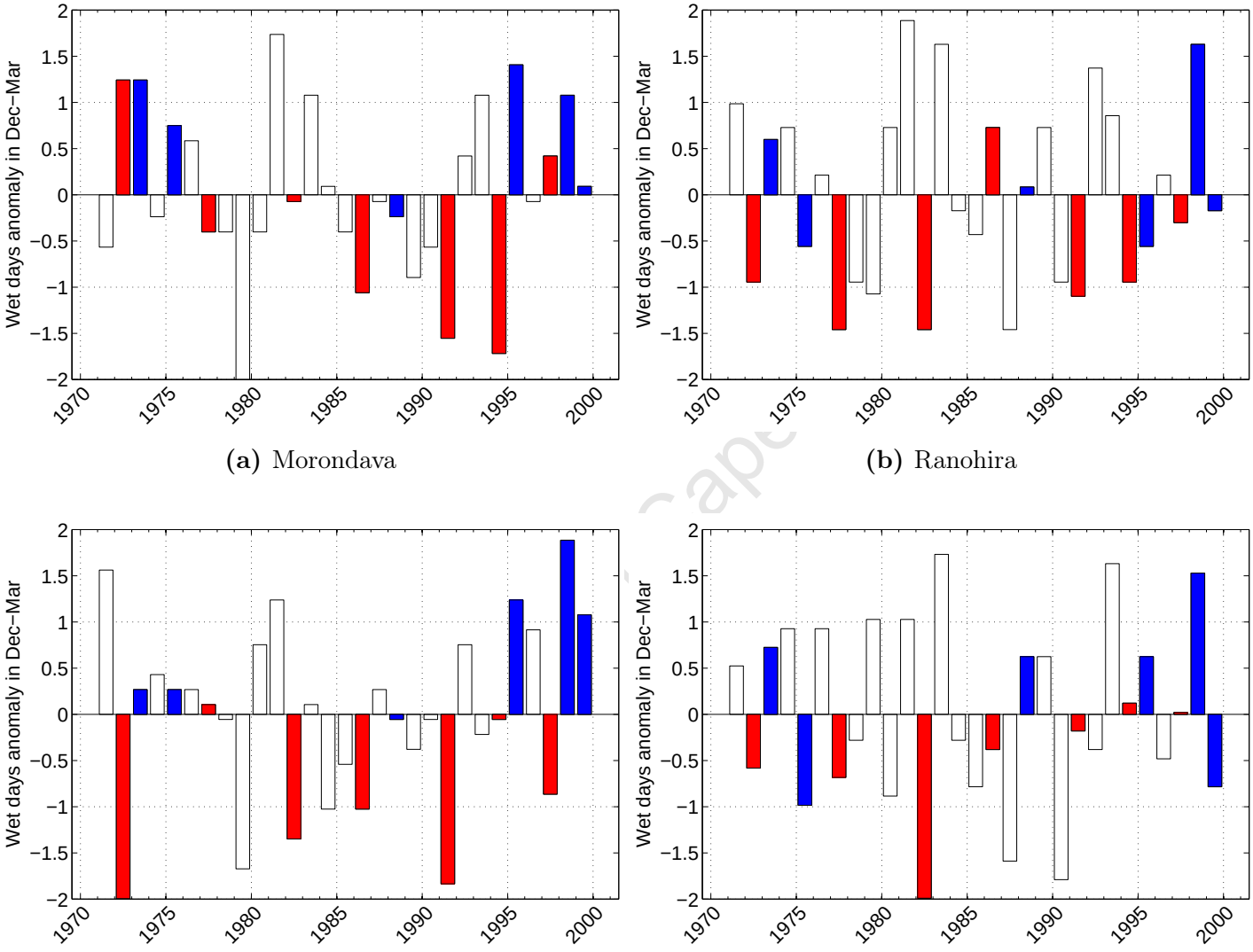

(a) Morondava **(b)** Ranohira

(c) Toliara **(d)** Taolagnaro

Figure 3.4: Standardised anomalies of the frequency of wet days for Dec–Mar at the four stations. The red bars correspond to El Niño seasons and the blue bars correspond to La Niña seasons (El Niño and La Niña years are based on the Oceanic Niño Index at `http://www.cpc.ncep.noaa.gov`).

Station name	High frequency of wet days	Type	Low frequency of wet days	Type
Morondava	1972-73	El Niño	1979–80	
	1973–74	La Niña	1986–87	El Niño
	1981–82		1991–92	El Niño
	1983–84		1994–95	El Niño
	1993–94			
	1995–96	La Niña		
	1998–99	La Niña		
Ranohira	1971–72		1977–78	El Niño
	1981–82		1979–80	
	1983–84		1982–83	El Niño
	1992–93		1987–88	
	1998–99	La Niña	1991–92	El Niño
Taolagnaro	1979–80		1975–76	La Niña
	1981–82		1982–83	El Niño
	1983–84		1987–88	
	1993–94		1990–91	
	1998–99	La Niña		
Toliara	1971–72		1972–73	El Niño
	1981–82		1979–80	
	1995–96	La Niña	1982–83	El Niño
	1998–99	La Niña	1984–85	
	1999-2000	La Niña	1986–87	El Niño
			1991–92	El Niño

Table 3.1: Wettest and driest rainy seasons at the four stations according to their the frequency of wet days for Dec–Mar.

3.3 Extreme events for composite analyses

Among the years characterized by an anomalously high frequency of wet days for the four stations, are the four La Niña seasons: 1973–74, 1995–96, 1998–99, 1999–00. Years having anomalously low frequency of wet days occurring with El Niño events are 1972–73, 1977–78, 1982–83, 1986–87, 1991–92, 1994–95.

This result suggests that La Niña events are often associated with increased number of wet days in southwestern Madagascar. El Niño events might reduce the number of wet days in the region. The most common wet years are: 1981–82 (neutral year for ENSO, positive phase of SIOD) and 1998–99 (La Niña year) for the four stations. The most common dry years are: 1979–80 (neutral year) and 1991–92 (El Niño year) except for Taolagnaro station located in the east coast. Table 3.2 summarizes the years used for composites analysis.

El Niño seasons	1972–73, 1977–78, 1982–83, 1986–87, 1991–92, 1994–95, 1997–98
La Niña seasons	1973–74, 1975–76, 1988–89, 1995–96, 1998–99, 1999–00
Wettest seasons	1981–82 (neutral), 1998–99 (La Niña)
Driest seasons	1979–80 (neutral), 1991–92 (El Niño)

Table 3.2: Seasons used for composite analyses.

3.4 Correlation of the frequency of wet days with climate indices

Previous studies have found that several regions remote from the Pacific Ocean basin such as Australia, North America, South America, Africa, Central America have precipitation patterns associated with ENSO (Ropelwski, 1987). Also, enhanced rainfall over large areas of southeastern Africa occurs with positive phase of SIOD (Reason, 2001). This section investigates the possible relationship that may exist between ENSO, SIOD and the anomaly of the frequency of wet days over southwestern Madagascar.

The correlation coefficients between ENSO indices, SIOD index and the anomaly of the

frequency of wet days at the four stations studied, is summarized by Table 3.3. Only correlation coefficients which are statistically significant at the 90% confidence level are shown in the table.

The correlation between the anomaly the frequency of wet days and SOI are all positive at the four stations as shown in Table 3.3. The correlation is much stronger at Toliara, $r = 0.597$ and $p = 0.0008$. At the three other stations, the correlation is weak $r \simeq 0.350$ and $p \leq 0.1$. These results suggest a direct relationship between sea level pressure in the eastern Pacific and the frequency of wet days in southwestern Madagascar.

Negative correlation coefficients are found for Niño1+2, Niño3, Niño3.4 at all stations (Table 3.3). That would suggest an inverse relationship between SST anomaly in equatorial Pacific and the anomaly of the frequency of wet days in southwestern Madagascar. Correlation between the time series of the frequency of wet days in summer at Toliara and the record of summer mean Niño3.4 SST anomalies is $r = -0.612$ with $p = 0.0005$, confirming that El Niño influences significantly summer rainfall over Toliara region. Strong correlations are also obtained between Niño1+2, Niño3, Niño4 SST anomalies and the frequency of wet days at Toliara as shown in Table 3.3d. The results are statistically significant at the 95% confidence level and would suggest that drought years over Toliara are often but not exclusively related to the warm SST anomalies (El Niño) in the equatorial central and eastern Pacific. Whereas, wet years are associated with anomalously cold SSTs (La Niña). The corresponding statistics of this result is shown clearly in Table 3.1. Some of the years having low frequency of wet days correspond to El Niño seasons. Inversely, anomalously high frequency of wet days is associated with La Niña seasons. However, dry years (wet years) are possible in southwestern Madagascar even if there is no El Niño (La Niña), as seen in Figure 3.4. Therefore, factors other than ENSO may also influence rainfall variations in the region.

Correlations between SDI and the anomaly of the frequency of wet days in southwestern Madagascar are all positive for three stations: Ranohira, Toliara and Morondava (Table 3.3). Thus a direct relationship may exist between SIOD and the frequency of wet days in summer in the area of study. A strong relationship is found at Ranohira and Toliara, $r = 0.541$ and $r = 0.567$ respectively with $p \leq 0.05$. The result is consistent with the spatial correlation between the frequency of wet days at these two stations and SST in the subtropical Indian Ocean (between 40°S to 30°S and 60°E to 75°E), seen in Figure 3.5b and d. Correlation between the frequency of wet days at Morondava station and SDI is weak,

Index	r	p
SOI	0.367	0.0549
Niño4	-0.435	0.0208
SID	0.384	0.0439

(a) Morondava

Index	r	p
SOI	0.350	0.0678
Niño3.4	-0.379	0.0464
Niño3	-0.329	0.0877
SDI	0.541	0.0300

(b) Ranohira

Index	r	p
SOI	0.342	0.0747
Niño4	-0.325	0.0914

(c) Taolagnaro

Index	r	p
SOI	0.597	0.0008
Niño12	-0.511	0.0055
Niño3.4	-0.612	0.0005
Niño3	-0.579	0.0012
Niño4	-0.503	0.0064
SDI	0.567	0.0017

(d) Toliara

Table 3.3: Correlation coefficients r between time series of the frequency of wet days during Dec–Mar and SOI, SDI, Niño12, Niño3.4, Niño3, Niño4 averaged over the same season for $p \leq 1$. The years of the time series are from 1971 to 2000.

$r = 0.384$ with $p = 0.0439$. Correlation between the frequency of wet days at Taolagnaro and SDI is not significant (not shown in Table 3.3c). Consequently, for Ranohira, Toliara and Morondava, number of wet days above (below) average may be associated with positive (negative) phase of SIOD. Apparently SST variations in the subtropical southern Indian Ocean have strong influence on summer rainfall over southwestern Madagascar. This result is confirmed by the previous work on subtropical SST dipole events in southern Indian Ocean (Behera and Yamagata, 2001); less precipitation occurs over southern Madagascar during the negative phase of SIOD.

3.5 Spatial correlations of the frequency of wet days with fields

3.5.1 Spatial correlations of the frequency of wet days with SST

Tropical Pacific Ocean

In its normal state, the tropical Pacific Ocean is dominated by warm SST in the western part and cold SST in the eastern part. Ascending mass of air over the region of warm water is characterised by low pressure at the surface and precipitation, while subsidence and dry atmosphere occur over the region of cold water. During El Niño, anomalously warm SST replaces the cold water in the eastern equatorial Pacific. Eastward displacement of the convective zone enhances heavy rainfall over southeastern tropical Pacific. The opposite pattern happens during La Niña: Strengthening of the trade winds favours strong cooling of SST in the central and eastern tropical Pacific. The region of persistent precipitation shifts westward to western Australia and Indonesia (Philander, 1990; Sarachik and Cane, 2010).

Interannual variations of summer rainfall over Toliara region are strongly influenced by El Niño episodes in the Pacific Ocean as it was discussed in Section 2.2. The teleconnection pattern between the frequency of wet days in summer at Toliara and the tropical SST (Figure 3.5d) is dominated by strong negative correlations (statistically significant at the 90% level) in the eastern Pacific extending to the coast of Ecuador and Peru, and strong positive correlations in the western Pacific. It confirms the strong impact of El Niño on summer rainfall over Toliara and is consistent with the relationship found between the anomaly of the frequency of wet days at Toliara and Niño1+2, Niño3, Niño3.4 and Niño4 SST anomalies (Table 3.3d). However, spatial correlations with global SST (significant at the 90% level) are much weaker in the tropical Pacific for the three other stations: Ranohira, Morondava, Taolagnaro as shown in Figure 3.5a,b,c.

The frequency of wet days in summer at Ranohira has weak negative correlation with the tropical Pacific SST between 5°S to 5°N and 150°E to 160°W (Figure 3.5b). This spatial correlation is consistent with the correlation between the frequency of wet days of the station and the Niño3.4 SST anomaly discussed in the previous section.

Correlation between the frequency of wet days at Morondava station and SST field is negative in the region between 5°S to 5°N and 165°E to 150°W (Figure 3.5a). This is consistent with the negative correlation between Niño4 SST anomaly and the frequency of wet days at this station (Table 3.3a).

The region of negative spatial correlation with global SST is smaller for Taolagnaro station, between 5°N to 5°S and 170°E to 165°W which is included in Niño4 region (Figure 3.5c). The result is consistent with correlation between the frequency of wet days of this station and Niño3 SST anomaly.

Indian Ocean

SST in the southern Indian Ocean is highly correlated with summer rainfall over Ranohira and Toliara regions. A positive correlation is seen between 40°S to 30°S and 55°E to 70°E (west pole of SIOD) and negative correlation is seen between 20°S to 10°S at 55°E and 28°S to 20°S at 105°E which includes the east pole of SIOD (Figure 3.5b,d). This observation is confirmed by the positive correlations between SDI and the frequency of wet days at Ranohira and Toliara, seen in Table 3.3b,d. Thus positive phase of SIOD may be associated with increased number of wet days in these two stations.

A strong negative correlation between the frequency of wet days at Taolagnaro and SST is seen in the south of Madagascar, stretching across Mozambique Channel (Figure 3.5c). It would suggest that enhanced evaporation located over these regions might cause cooling of SST during the period of high frequency of wet days at Taolagnaro station.

3.5.2 Spatial correlations of the frequency of wet days with 850 hPa geopotential height

Previous studies by Sir Gilbert Walker at the beginning of the 20th century, to predict interannual variations of the monsoon showed that surface pressure over the Indian Ocean and over the eastern tropical Pacific are out of phase: an occurrence of high pressure in the eastern Pacific is associated with an occurrence of low pressure in the Indian Ocean extending from Africa to Australia (Philander, 1990). The negative correlations between the frequency of wet days at the four stations in southwestern Madagascar and the 850 hPa

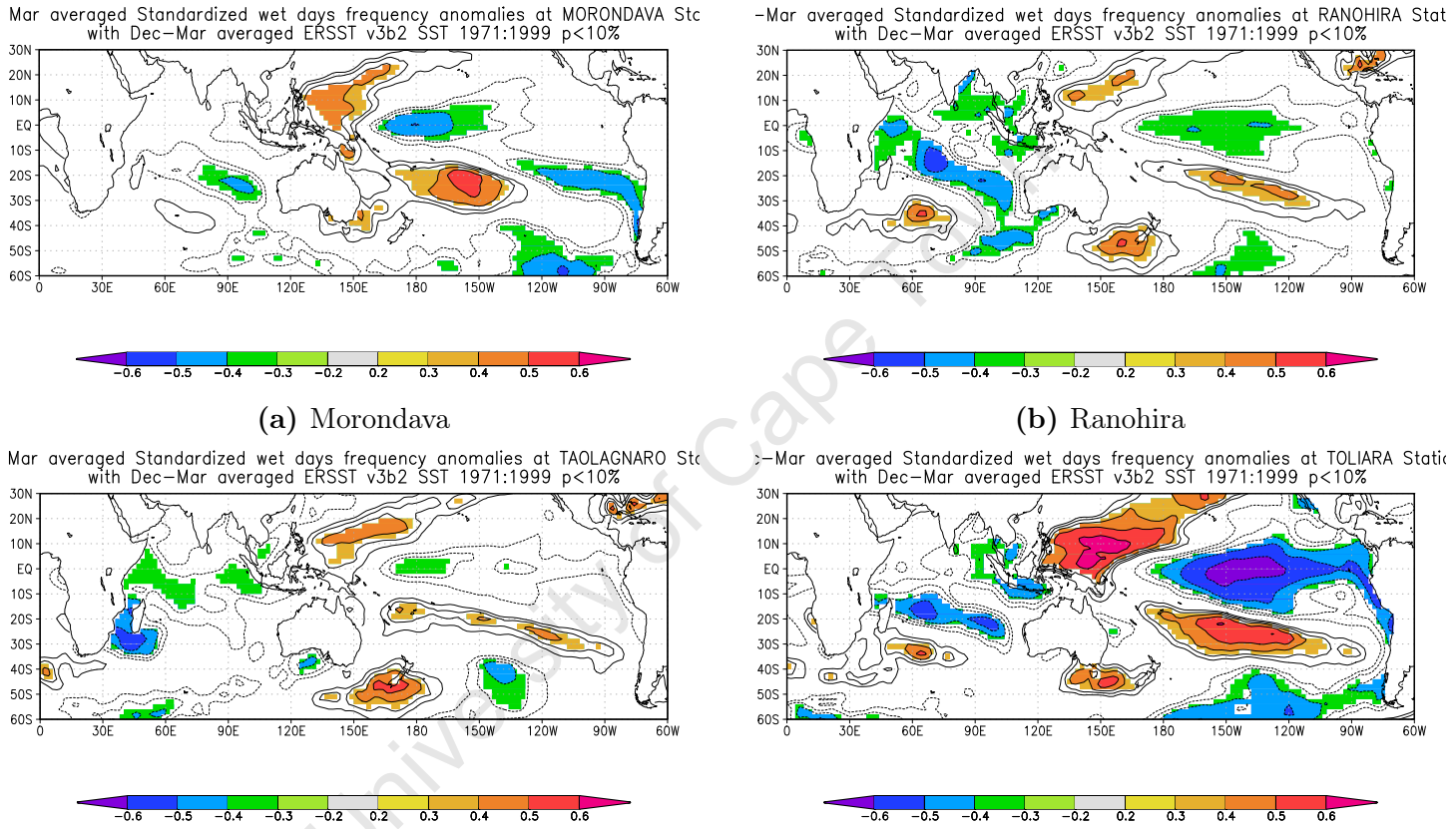

(a) Morondava **(b)** Ranohira

(c) Taolagnaro **(d)** Toliara

Figure 3.5: Correlation map of the frequency of wet days with SST for Dec–Mar of 1971–2000. Solid contours (dashed contours) correspond to positive value (negative value) while the shaded areas correspond to significance at the 90% level.

geopotential height extending across tropical Atlantic, Africa, Indian Ocean and western Pacific seem to be a La Niña signal (Figure 3.6). The pattern is more pronounced for the correlation with the number of wet days at Toliara station (Figure 3.6d). Increased rainfall over southwestern Madagascar may be associated with decreased surface pressure in the tropical Indian Ocean and the western Pacific during La Niña, which is consistent with the correlations between the number of summer wet days and ENSO indices.

At Toliara station, correlation of the frequency of wet days with 850 hPa geopotential height shows a strong negative correlation in south Atlantic Ocean, southern Africa and south Pacific Ocean extending to Australia, Indonesia and New Guinea (Figure 3.6d). The result would suggest that high frequency of wet days at this rainfall station could be associated with low atmospheric pressure over these areas.

For Morondava station, a weak negative correlation is observed over south Atlantic Ocean, most of southern Africa and the north of Australia (Figure 3.6a). It would suggest that low atmospheric pressure over these regions may occur during years having high frequency of wet days at Morondava, or inversely, high atmospheric pressure over these regions may be associated with low frequency of wet days at this station.

Similar to that of Morondava, a weak negative correlation between the frequency of wet days at Ranohira station and 850 hPa geopotential height is observed in south Atlantic Ocean, southern Africa and south Pacific Ocean stretching across northwestern Australia and Indonesia. The negative correlation is much stronger over the southern Madagascar extending to the southern Mozambique Channel (Figure 3.6b). A strong negative correlation is also shown in the southern Mozambique Channel for Toliara and Taolagnaro stations (Figure 3.6c,d). It may suggest that low pressure system over the southern Mozambique Channel favours increased frequency of wet days in southwestern Madagascar. A strong cyclonic circulation associated with clouds band might also occur in southern Mozambique Channel during the summer season having anomalous high frequency of wet days in southwestern Madagascar.

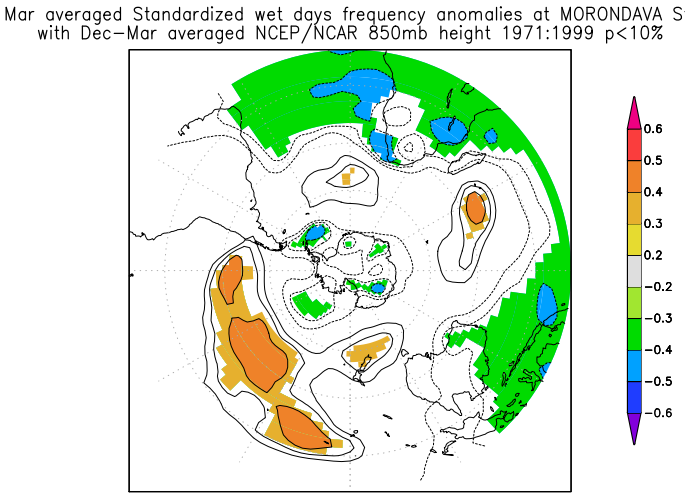

(a) Morondava

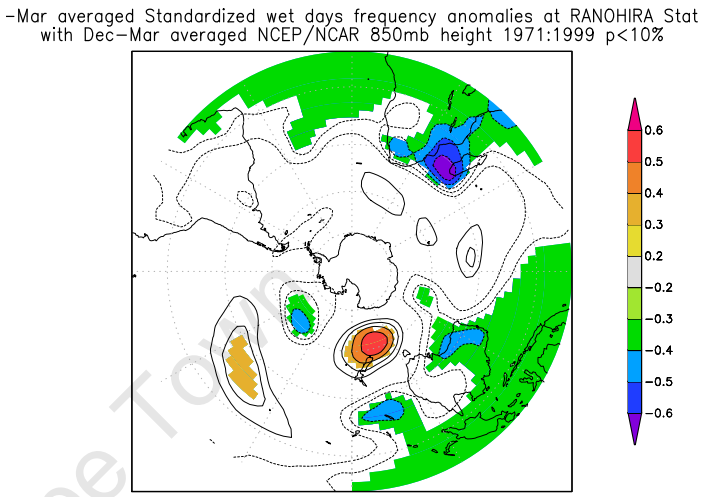

(b) Ranohira

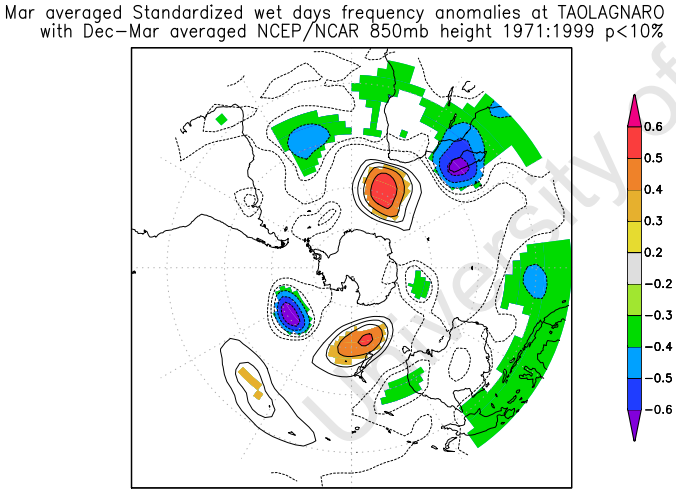

(c) Taolagnaro

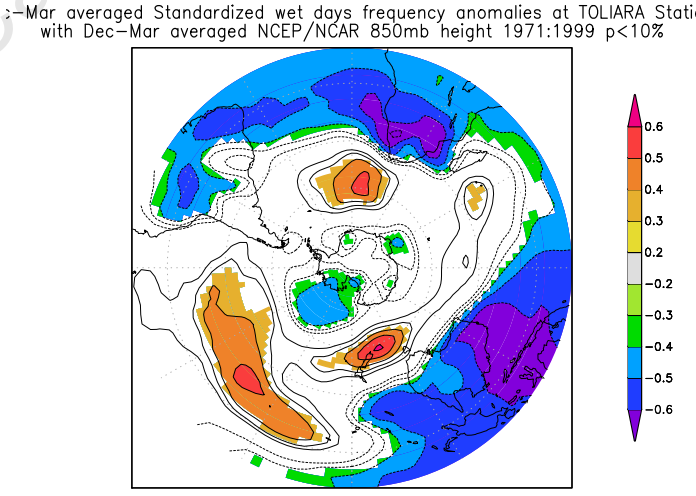

(d) Toliara

Figure 3.6: Correlation map of the frequency of wet days with geopotential height for Dec–Mar of 1971–2000. Solid contours (dashed contours) correspond to positive value (negative value) while the shaded areas correspond to significance at the 90% level.

3.5.3 Spatial correlations of the frequency of wet days with zonal and meridional winds at the surface

The correlation maps between the frequency of wet days at Morondava, Ranohira, Toliara and zonal wind at the surface (Figures 3.7a,b,d) shows a positive correlation between 20°S and 10°S. The correlation is much stronger between 60°E and 70°E for Morondava and Toliara as shown in Figures 3.7a,d. The observation would suggest that increased number of wet days in southwestern Madagascar may be related to the occurrence of westerly monsoonal wind over the northeast of Madagascar during summer. A negative correlation between the frequency of wet days at Morondava, Ranohira, Toliara and the meridional wind at the surface is seen between 25°S and 10°S (Figure 3.8a,b,d).

It would suggest that a northerly wind over this region is associated with increased frequency of wet days in southwestern Madagascar. While positive correlation between the frequency of wet days at these three stations and the meridional wind from about 30°S to 15°S may suggest a southerly wind associated with increased frequency of wet days. In summary, the correlation between the frequency of wet days at the three stations (Morondava, Ranohira and Toliara) and the meridional wind circulation (Figure 3.8a,b,d) may suggest that increased number of wet days in southwestern Madagascar is associated with the southward displacement of the ITCZ during southern hemisphere summer.

The correlations observed for Taolagnaro station are different from the three other stations(Figures 3.7c and 3.8c). A weak positive correlation between the frequency of wet days and the zonal wind is shown in the south of Madagascar. The correlation is much stronger in the southern Mozambique Channel near the southwestern coast of Madagascar (Figure 3.7c). While, correlation between the frequency of wet days at Taolagnaro and the meridional wind at the surface is negative in the south of Madagascar and in the southern Mozambique. The result would suggest that moist air from local evaporation of warm SST just in the south of Madagascar is transported by northwesterly winds from the southern Mozambique Channel toward Taolagnaro region. Cold SST may result after evaporation, consistent with the negative correlation between the the frequency of wet days at Taolagnaro station and SST in the south of Madagascar seen in Figure 3.5c. Therefore enhanced rainfall implies anomalously high frequency of wet days at Taolagnaro.

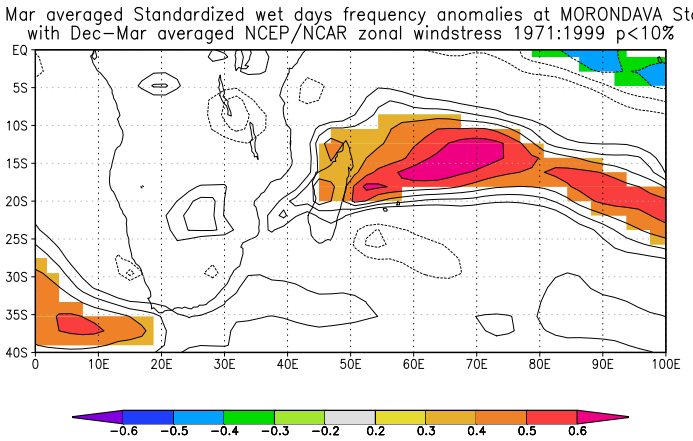

(a) Morondava

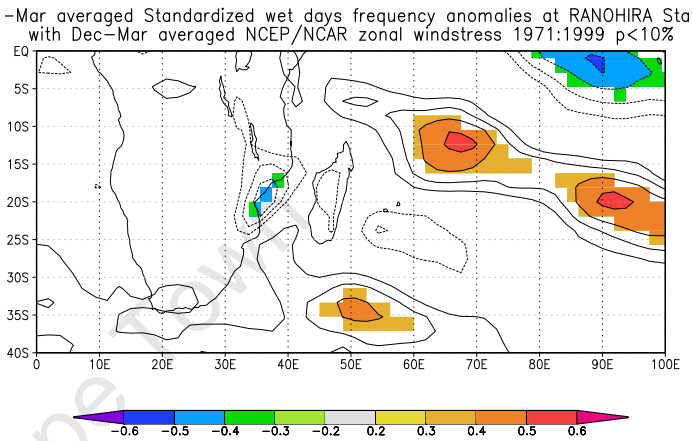

(b) Ranohira

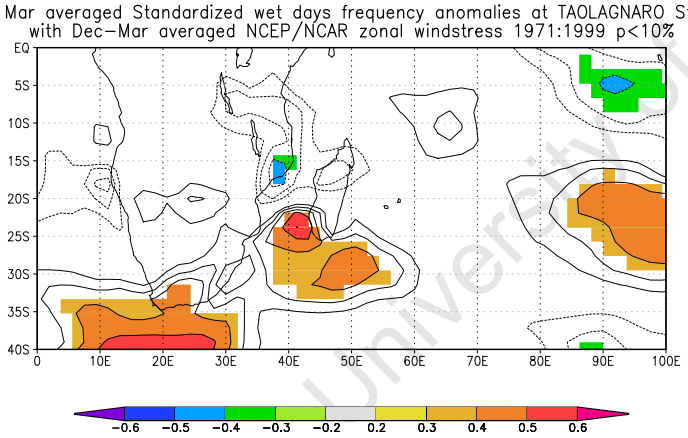

(c) Taolagnaro

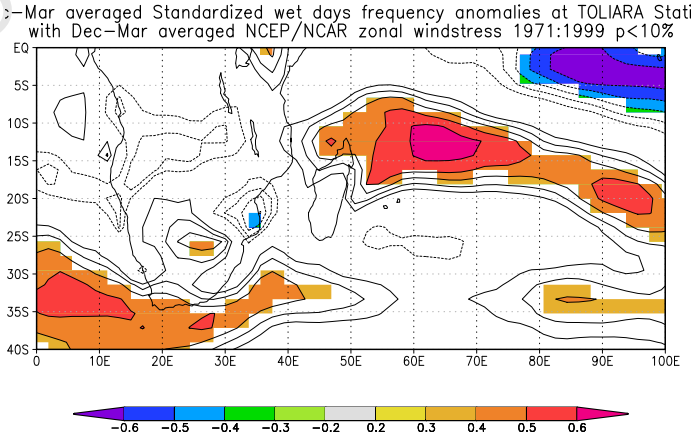

(d) Toliara

Figure 3.7: Correlation map of the frequency of wet days with zonal wind for Dec–Mar of 1971–2000. Solid contours (dashed contours) correspond to positive value (negative value) while the shaded areas correspond to significance at the 90% level.

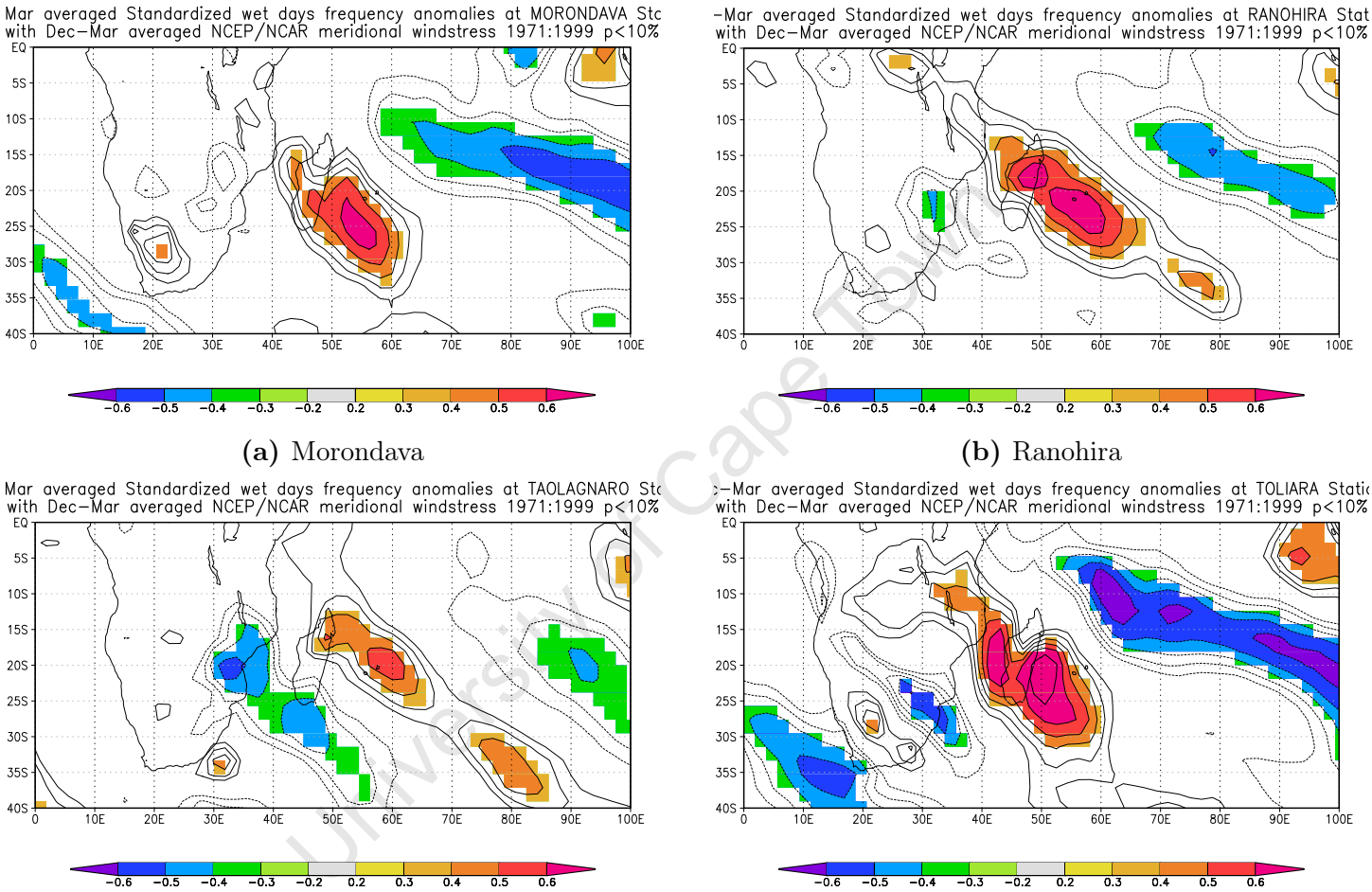

(a) Morondava

(b) Ranohira

(c) Taolagnaro

(d) Toliara

Figure 3.8: Correlation map of the frequency of wet days with meridional wind for Dec–Mar of 1971–2000. Solid contours (dashed contours) correspond to positive value (negative value) while the shaded areas correspond to significance at the 90% level.

Chapter 4

Composite analyses

4.1 Climatology

4.1.1 Moisture flux and moisture flux convergence at 850 hPa

The long term mean of the moisture flux and the moisture flux convergence at 850 hPa pressure level over the period of 1971 to 2000, seen in Figure 4.1 (note that the moisture flux convergence is represented by the negative divergence field of moisture flux), shows a cyclonic circulation over the Mozambique Channel which converges strongly in the centre of the channel. A strong import of moist air, transported by the northeasterly monsoon, is seen over southeastern Kenya. It converges strongly over western Tanzania. An appearance of the northwesterly monsoon is seen over the northwest of Madagascar. A large area of cyclonic circulation is shown over the tropical western Indian Ocean, it is associated with strong convergence in the centre. This cyclonic circulation is reinforced by the southeasterly trade wind in its southern edge and by the reversal monsoon wind in its northern edge. Whilst, a large area of anticyclonic circulation associated with weak divergence is observed in south Indian Ocean which is the permanent subtropical anticyclone. In the boundary between the two large cyclonic and anticyclonic circulations, situated in the central Indian Ocean, an easterly circulation originates from the eastern Indian Ocean at about 20°S. It reaches eastern Madagascar and recurves to the south to join southeastern African land masses. The circulation diverges strongly over northeastern South Africa where a source

region of water vapour is observed.

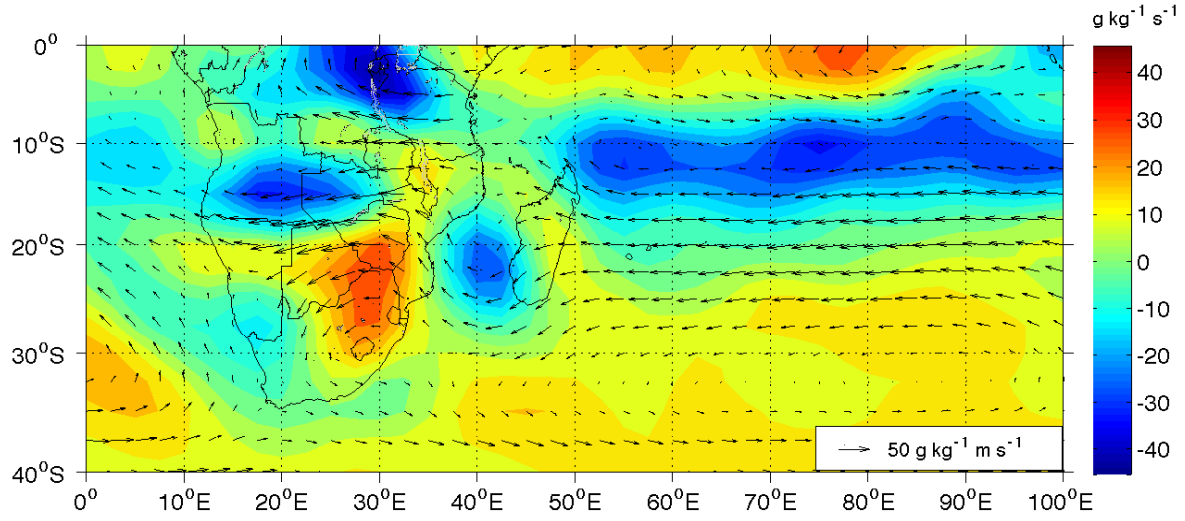

Figure 4.1: Climatology of moisture flux (vector) and moisture flux divergence (shaded) for Dec–Mar of 1971–2000.

4.1.2 Omega at 500 hPa

In Figure 4.2, a large band with negative value of the omega at 500 hPa pressure level is observed between about 10°S to 20°S and 15°E to 100°E. It indicates an ascent of wind at mid-level in the regions overlaid by the band. A weak negative omega is seen over South Africa, suggesting a slow ascent of a mass of air at 500 hPa. Whilst, a weak positive 500 hPa omega seen in the subtropical Indian Ocean corresponds to a slow descent of air masses over the region, consistent with the presence of the subtropical anticyclone. The climatology of 500 hPa omega (Figure 4.2) is consistent with the mean circulation of moisture flux and moisture flux convergence at 850 hPa pressure level. The mean circulation suggests that the central western Indian Ocean was dominated by a centre of low pressure system associated with an ascent of air masses at mid-level and a strong convergence at 850 hPa, during the period of 1971 to 2000. Whilst, subsidence often occurred in the subtropical Indian Ocean.

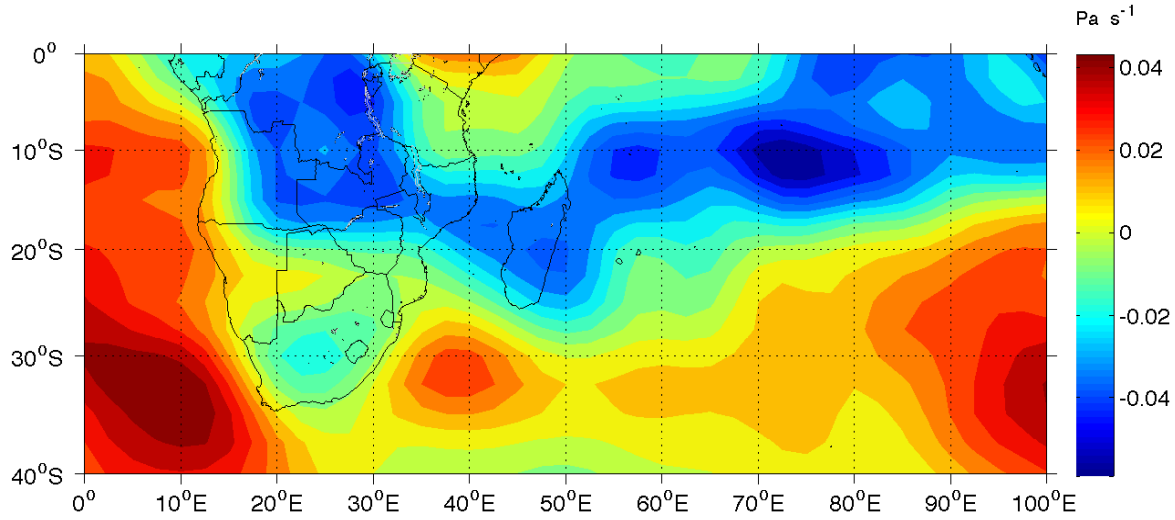

Figure 4.2: Climatology of 500 hPa omega for Dec–Mar of 1971–2000.

4.1.3 Velocity potential at .995 sigma level

In Figure 4.3, the long term mean of the velocity potential at .995 sigma level from 1971 to 2000 shows a positive velocity potential in the tropical Indian Ocean, Madagascar and southeastern Africa. The climatology plot suggests that the mean circulation of the Walker cell is characterized by a rising branch over these regions. The negative velocity potential observed in the tropical eastern Atlantic suggests a descending branch of the Atlantic Walker cell.

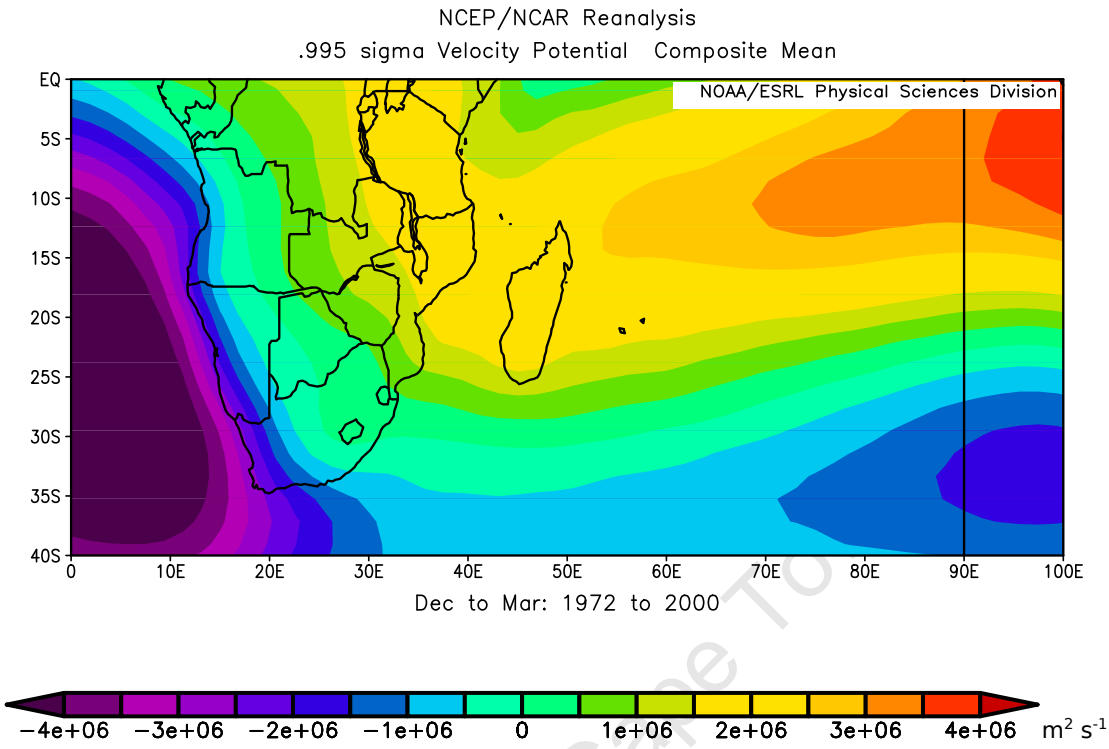

Figure 4.3: Climatology of velocity potential at .995 sigma level for Dec–Mar of 1971–2000.

4.2 Circulation anomaly

4.2.1 Moisture flux and moisture flux convergence at 850 hPa

During the El Niño events occurring between 1971 and 2000, anomaly plot of the moisture flux and moisture flux convergence at 850 hPa pressure level in Figure 4.4 shows that southern Madagascar is a zone of transition between an anticyclonic circulation anomaly associated with weak divergence, stretching over southern Mozambique Channel to southern Mozambique and Zimbabwe; and a large cyclonic anomaly associated with weak convergence in the east of Madagascar. Consequently, a southerly moisture flux anomaly flow over southern Madagascar during the El Niño seasons. In addition, a strong anticyclonic circulation anomaly diverges strongly over the central western Indian Ocean during these seasons.

Circulation anomaly of the moisture flux and the moisture flux convergence at 850 hPa pressure level during La Niña periods occurring between 1971 and 2000 (Figure 4.5) shows a

source region of water vapour in the east of Madagascar. A weak divergence is observed over this region. Thus a northeasterly moisture flux anomaly converges weakly over southern Madagascar extending just to the south of the island. A strong convergence of cyclonic anomaly is seen over the boundary between southwestern Zambia, southeastern Angola, northeastern Namibia and northwestern Botswana. A divergence of moist air is observed in the central northern South Africa causing a source of water vapour.

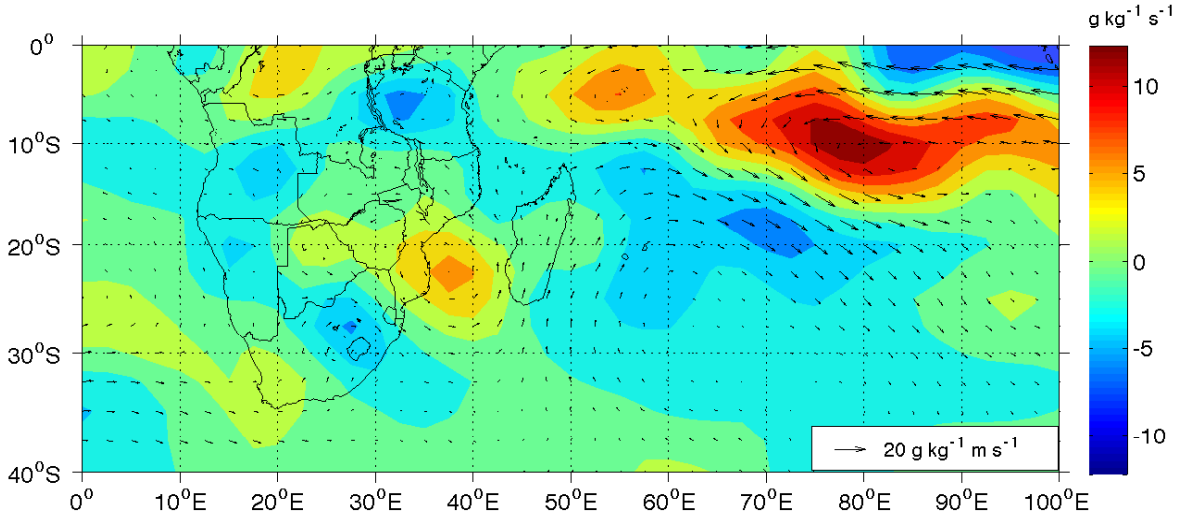

Figure 4.4: Composite anomalies of moisture flux (vector) and moisture flux divergence (shaded) of El Niño years (1972–73, 1977–78, 1982–83,1986–87,1991–92,1994–95,1997–98).

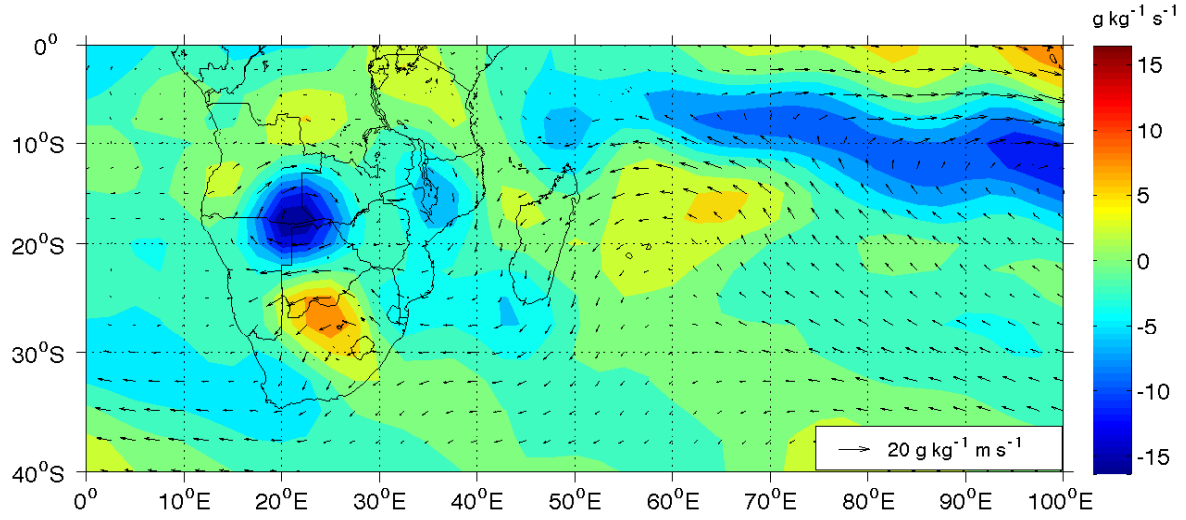

Figure 4.5: Composite anomalies of moisture flux (vector) and moisture flux convergence (shaded) of La Niña years (1973–74,1975–76,1988–89,1995–96,1998–99,1999–00).

During the season December 1979 to March 1980, having anomalously low frequency of wet days, two strong cyclonic anomalies are observed in the east of Madagascar (Figure 4.6). The first cyclonic anomaly is located just in the east of Madagascar and the second is situated in the central western Indian Ocean. They are characterized by strong negative anomaly of moisture flux divergence. In association with the cyclonic anomaly in the east of Madagascar, a southeasterly moisture flux anomaly is reinforced by the western edge of the cyclonic circulation anomaly over western Madagascar.

During the El Niño season 1991–92, a severe drought affected southern Madagascar (Randriamanga et al., 1995). In this study, it is confirmed that December 1991 – March 1992 is an El Niño season characterised by low frequency of wet days for Morondava, Ranohira and Toliara stations as shown in Figure 3.4a,b,c (1991–92 corresponds to a red bar) and in Table 3.1. Associated circulation anomaly of the moisture flux and moisture flux convergence at 850 hPa (Figure 4.7) shows a large cyclonic anomaly in the east of Madagascar. In association with the winds along the western edge of the cyclonic circulation, a westerly moisture flux anomaly from northern South Africa and southern Mozambique recurves to the north over the southern Mozambique Channel and southwestern Madagascar. Thus an occurrence of southerly moisture flux anomaly, associated with weak divergence in southwestern Madgascar, is observed over the entire Madagascar during the summer season of 1991–92.

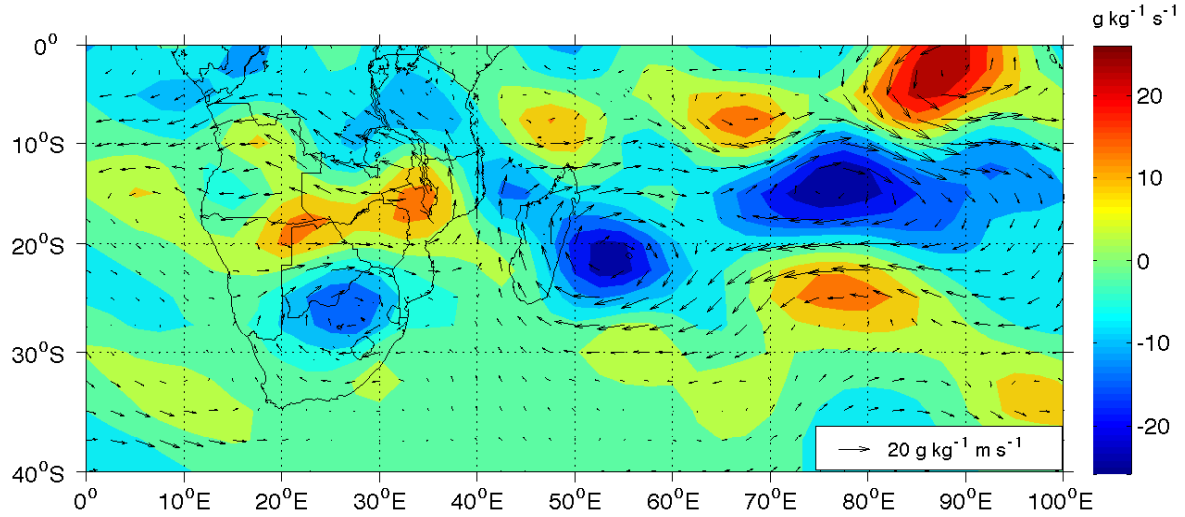

Figure 4.6: Anomalies of moisture flux (vector) and moisture flux convergence (shaded) for Dec 1979–Mar 1980 which is a neutral (non-ENSO) summer with low frequency of wet days.

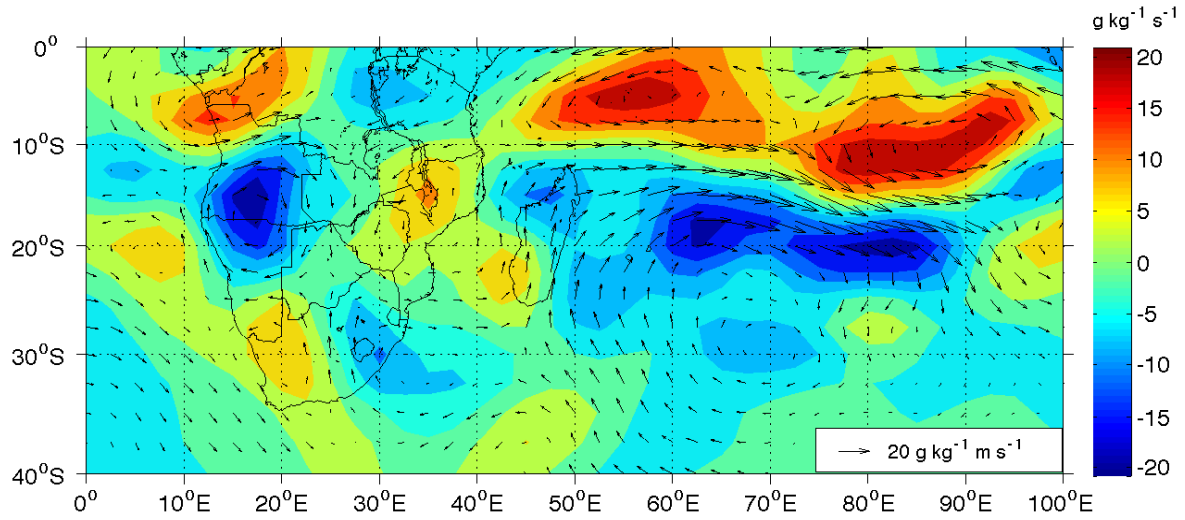

Figure 4.7: Anomalies of moisture flux (vector) and moisture flux convergence (shaded) for Dec 1991–Mar 1992 which is an El Niño summer season with low frequency of wet days.

During the wet season December 1981 to March 1982 southern Madagascar was a boundary between two anomalous circulations associated with strong convergence (Figure 4.8). The first circulation is a cyclonic anomaly over the Mozambique Channel. The second is a northwesterly moisture flux anomaly from Mozambique associated with a northeast-

erly moisture flux anomaly from Indian Ocean. The two northerly circulations converge strongly in the southeast of Madagascar at about 50°E. The anomalous circulations would suggest that an import of moisture into southern Madagascar may cause anomalously high frequency of wet days during the period of neutral (non-ENSO) wet season 1981–1982.

From December 1998 to March 1999, which is a La Niña season having high frequency of wet days in southwestern Madagascar (for the four stations studied, Figure 3.4 and Table 3.1), a strong export of moisture flux is seen in the east of Madagascar between about 15°S and 10°S. The easterly moisture flux anomaly recurves to the south over northern Mozambique and the northern Mozambique Channel. It reaches southwestern Madagascar as a northwesterly moisture flux anomaly associated with weak convergence. Thus increased frequency of wet days may result.

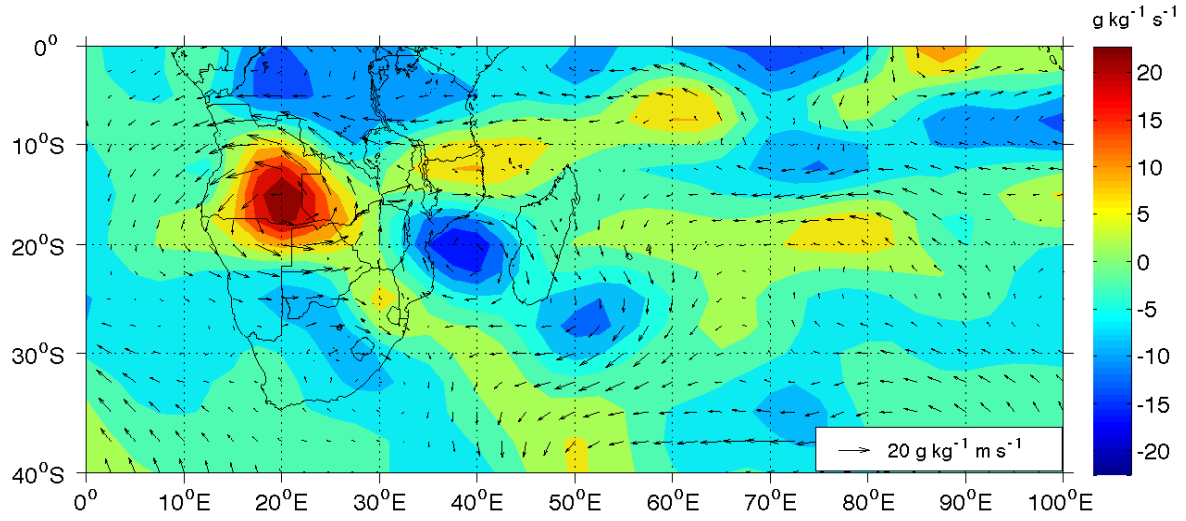

Figure 4.8: Anomalies of moisture flux (vector) and moisture flux convergence (shaded) for Dec 1981 – Mar 1982 which is a neutral (non-ENSO) summer season with high frequency of wet days.

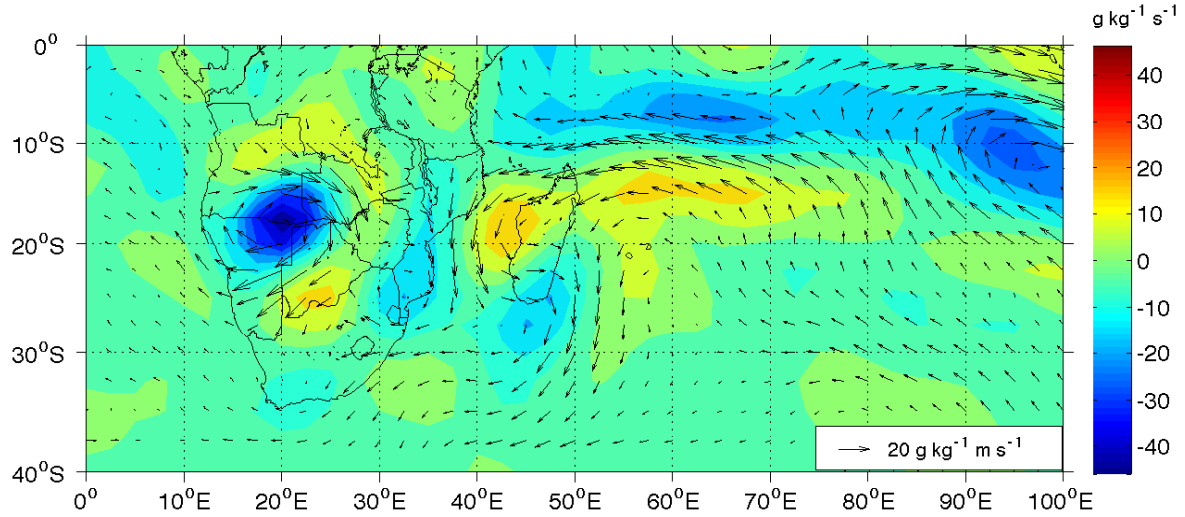

Figure 4.9: Anomalies of moisture flux (vector) and moisture flux convergence (shaded) for Dec 1998 – Mar 1999 which is a La Niña summer season with high frequency of wet days.

4.2.2 Omega at 500 hPa

During the El Niño seasons, a positive anomaly of omega at mid-level is observed over most regions of southern Africa including Madagascar, Figure 4.10. The anomaly is strongly positive over southern Mozambique, Zimbabwe, northeastern South Africa and eastern Botswana. The observation would suggest a relative descent of air masses at 500 hPa pressure level over southern Africa and Madagascar during the El Niño seasons between 1971 and 2000. While from about 60°E to 90°E, a negative anomaly of 500 hPa omega is observed. The anomaly is strongly negative between about 72°E and 85°E. A strong uplift wind at mid-level might occur over the warm pool of Indian Ocean during El Niño.

An overview of the 500 hPa omega circulation anomaly during La Niña seasons, Figure 4.5, shows the opposite pattern of the circulation anomaly occurring during El Niño seasons. During La Niña events, a weak negative anomaly of omega at mid-level is seen over Madagascar and Mozambique Channel. Whilst positive anomaly was observed in these regions during El Niño events (Figure 4.10). The anomaly during La Niña is strongly negative in northern South Africa and Botswana extending to the boundaries between Zimbabwe, Botswana, Zambia, Angola and Namibia. The composite anomaly during La Niña seasons may suggest a slow ascent of air masses at 500 hPa over Madagascar and Mozambique Channel; and a much stronger ascent over Botswana and northern South Africa. The op-

posite pattern of this circulation anomaly shifts slightly eastward during El Niño (Figure 4.10) and also the domain of anomaly is much larger than during La Niña. The circulation anomalies of omega at 500 hPa may explain the difference between the frequency of wet days in southwestern Madagascar during El Niño and that during La Niña. La Niña seasons tend to have above average number of wet days because of the relative ascent at mid-level occurring over Madagascar, which is a favourable condition for the increase of rainfall. A strong positive anomaly is observed in the Indian Ocean centred at 20°S and 70°E. The anomaly would suggest a strong descent of wind at 500 hPa over the warm pool of the Indian Ocean whereas a strong ascent occurs during El Niño.

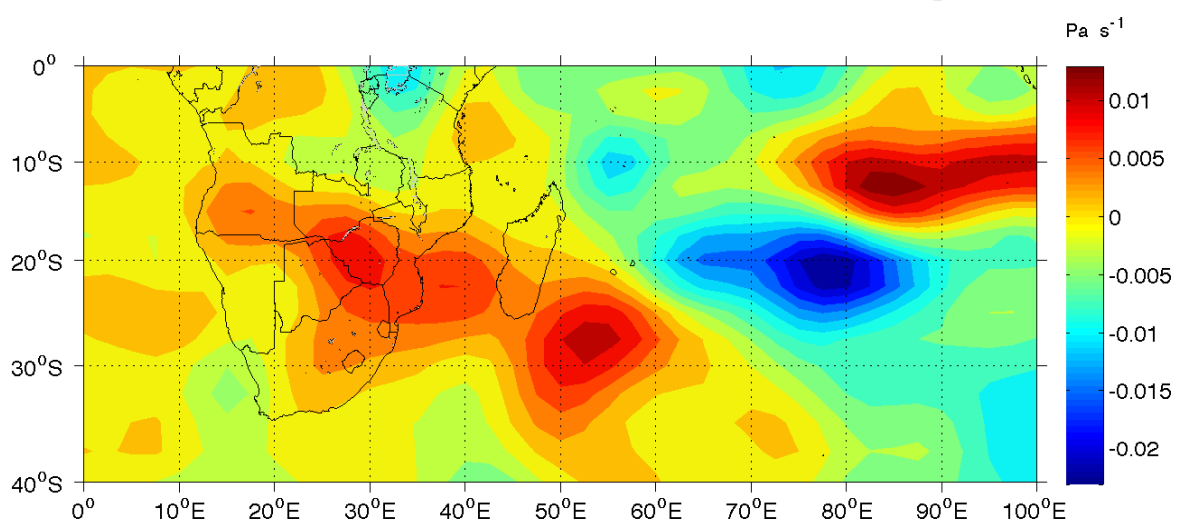

Figure 4.10: Composite anomaly 500 of hPa omega for Dec–Mar of El Niño years (1972–73, 1977–78, 1982–83,1986–87,1991–92,1994–95,1997–98).

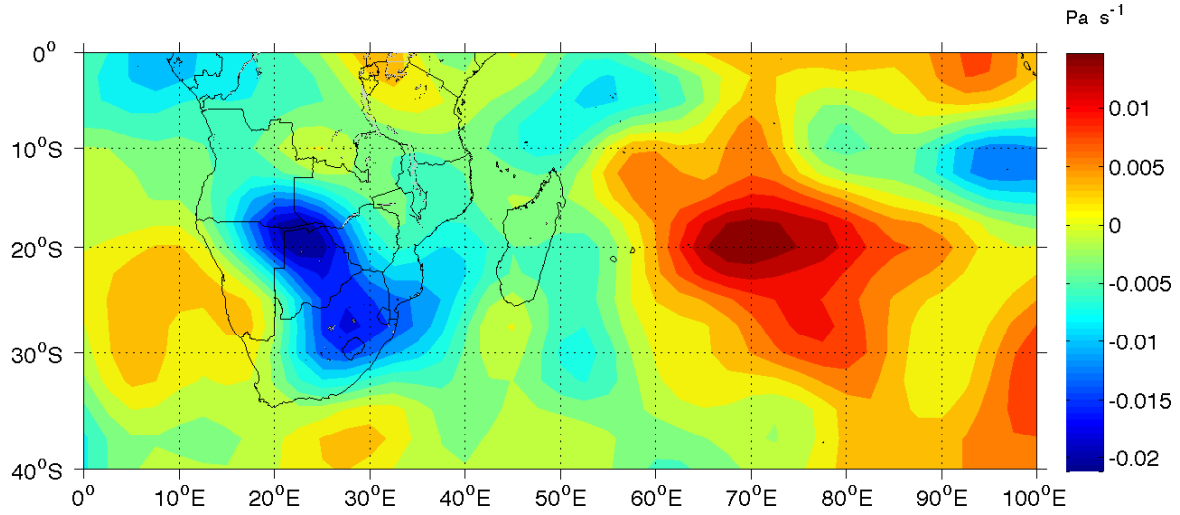

Figure 4.11: Composite anomaly of 500 hPa omega for Dec–Mar of La Niña years (1973–74,1975–76,1988–89,1995–96,1998–99,1999–00).

During the summer season December 1979 to March 1980, characterized by low frequency of wet days at Morondava, Ranohira and Toliara, a weak positive anomaly of 500 hPa omega is observed over most of Madagascar, Figure 4.12. A strong positive anomaly is seen over most of southeastern Africa and the Mozambique Channel. A relative descent of air masses at mid-level might occur over these regions during the neutral (non-ENSO) dry season 1979-1980. This condition may reduce the number of wet days in the regions of Morondava, Ranohira and Toliara. Whilst in the east of Madagascar, between 50°E and 100°E, a strong negative anomaly is observed. The anomaly would suggest a strong uplift wind at 500 hPa over this region of the Indian Ocean. This result is consistent with the two cyclonic circulation anomalies of moisture flux occurring in the east of Madagascar between 50°E and 100°E (Figure 4.6) during the same season.

A weak positive anomaly of omega at 500 hPa pressure level is shown over Madagascar, Mozambique Channel and southeastern Africa during the El Niño season 1991–92, seen in Figure 4.13. It may suggest a slow descent of air masses at mid-level over these regions. This condition favours decreased frequency of wet days in southwestern Madagascar. While a strong negative anomaly is shown in the Indian Ocean between 30°S to 10°S and 65°E to 85°E, implying a strong ascent at mid-level over the region.

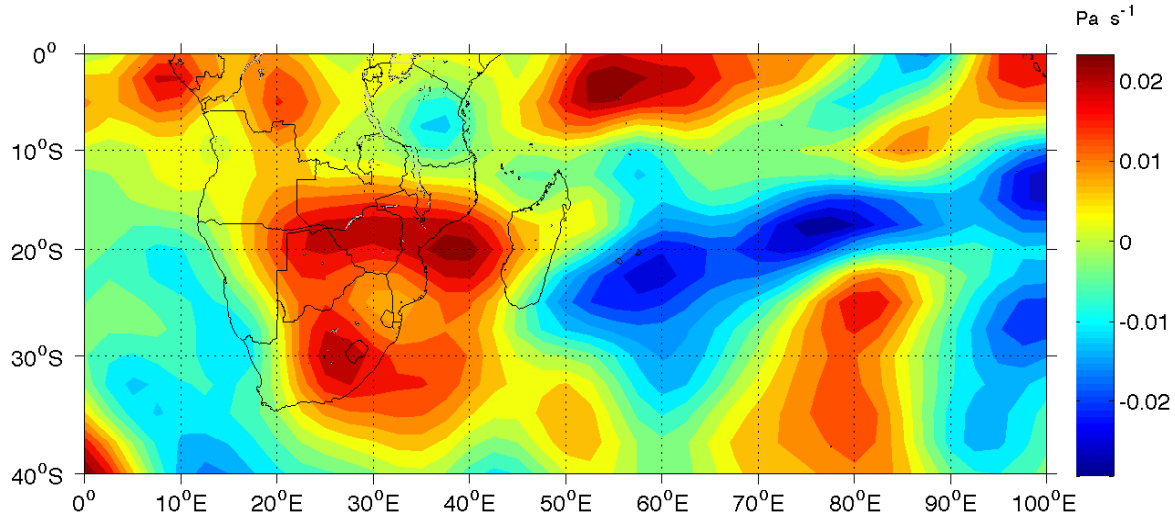

Figure 4.12: Anomalies of 500 hPa omega for Dec 1979–Mar 1980 which is a neutral (non-ENSO) summer season with low frequency of wet days.

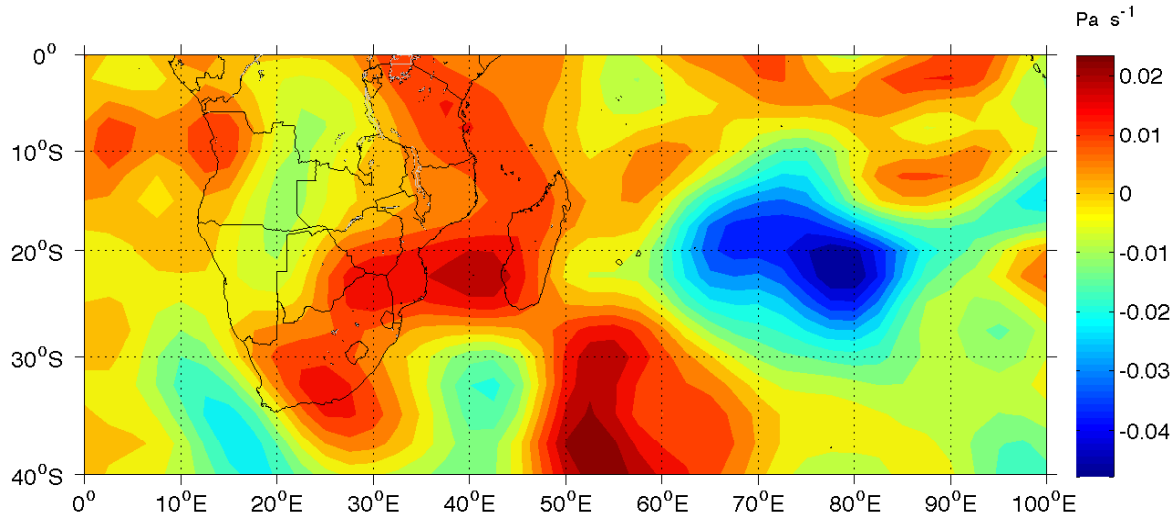

Figure 4.13: Anomalies of 500 hPa omega for Dec 1991–Mar 1992 which is an El Niño summer season with low frequency of wet days.

During the summer season December 1981 to March 1982, a season having anomalously high frequency of wet days in southwestern Madagascar (at the four stations), a negative anomaly of omega at 500 hPa is shown in the entire Madagascar (Figure 4.14). The anomaly is strongly negative in the southeast of Madagascar at about 60°E. It implies a relative ascent of air masses at 500 hPa over entire Madagascar during the neutral (non-ENSO) wet season 1981–82. While a strong positive anomaly of 500 hPa omega is seen

in northern South Africa and Botswana extending to the boundaries between Zimbabwe, Botswana, Zambia, Angola and Namibia. The anomaly may suggest a strong descent of wind at mid-level over these regions during the wet period of southwestern Madagascar. Similar circulation anomaly occurred in the north of Madagascar between 10°S and the Equator, the strong positive anomaly implies a relative descent of air masses at 500 hPa pressure level.

In Figure 4.15, a strong negative anomaly of 500 hPa omega is observed over southern Madagascar and southern Mozambique Channel during the La Niña episode 1998–99. The anomaly would suggest a strong ascent of air masses at 500 hPa pressure level over southern Madagascar, which is consistent with anomalous high frequency of wet days in southwestern Madagascar during the summer season December 1998–March 1999.

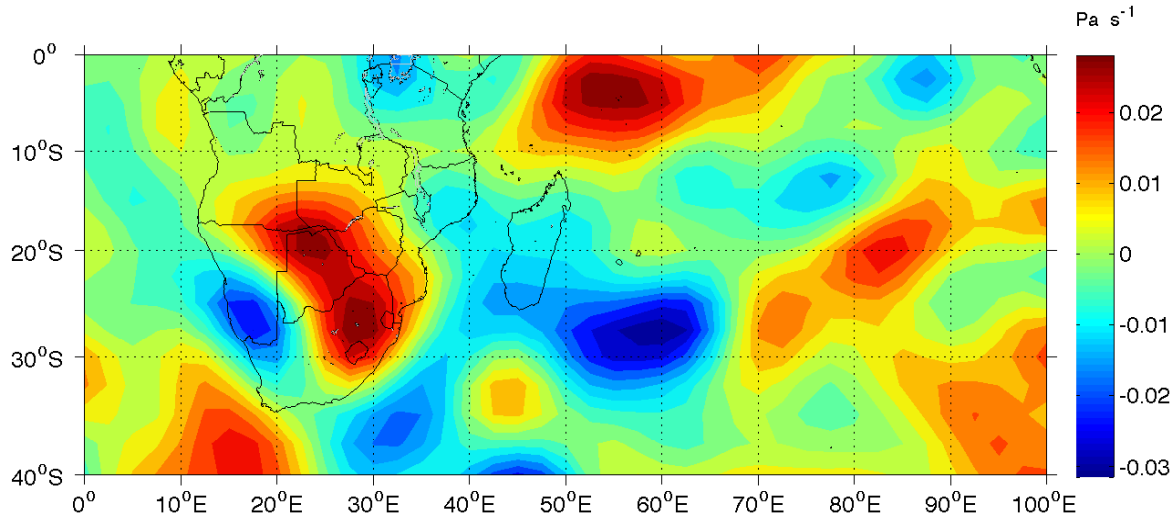

Figure 4.14: Anomalies of 500 hPa omega for Dec 1981–Mar 1982 which is a neutral (non-ENSO) summer season with high frequency of wet days.

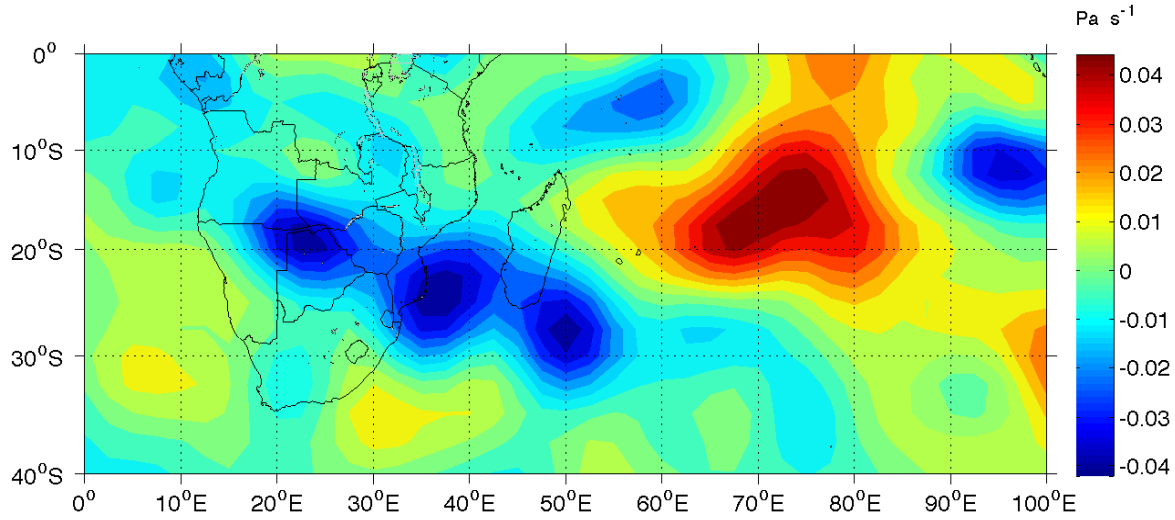

Figure 4.15: Anomalies of 500 hPa omega for Dec 1998–Mar 1999 which is a La Niña summer season with high frequency of wet days.

4.2.3 Velocity potential

The long term mean used for composite anomaly of .995 sigma velocity potential is over the period 1980 to 2010 as it is the climatology available in the NOAA monthly/seasonal climate composite website. During the El Niño seasons occurring between 1971 and 2000, anomaly of the velocity potential at .995 sigma level is positive in the east of Madagascar and weakly positive in most of southern Africa, as shown in Figure 4.16. It suggests a relative ascent of the branch of Walker circulation in the east of Madagascar during the El Niño seasons. A strong negative anomaly is observed in the tropical eastern Indian Ocean, suggesting an eastward relative descent of the western Pacific Walker cell.

In Figure 4.17, a positive anomaly of the velocity potential at low level is shown in the entire southern Africa and Madagascar during the La Niña events. The anomaly suggests that the ascending branch of the Walker circulation shifts westward during the periods of La Niña. This circulation anomaly is confirmed by previous study investigating the climatic signals of ENSO in the Indian Ocean (Reason et al., 2000), which concluded that ascending branch of the Walker circulation occurs over the African continent during La Niña phases.

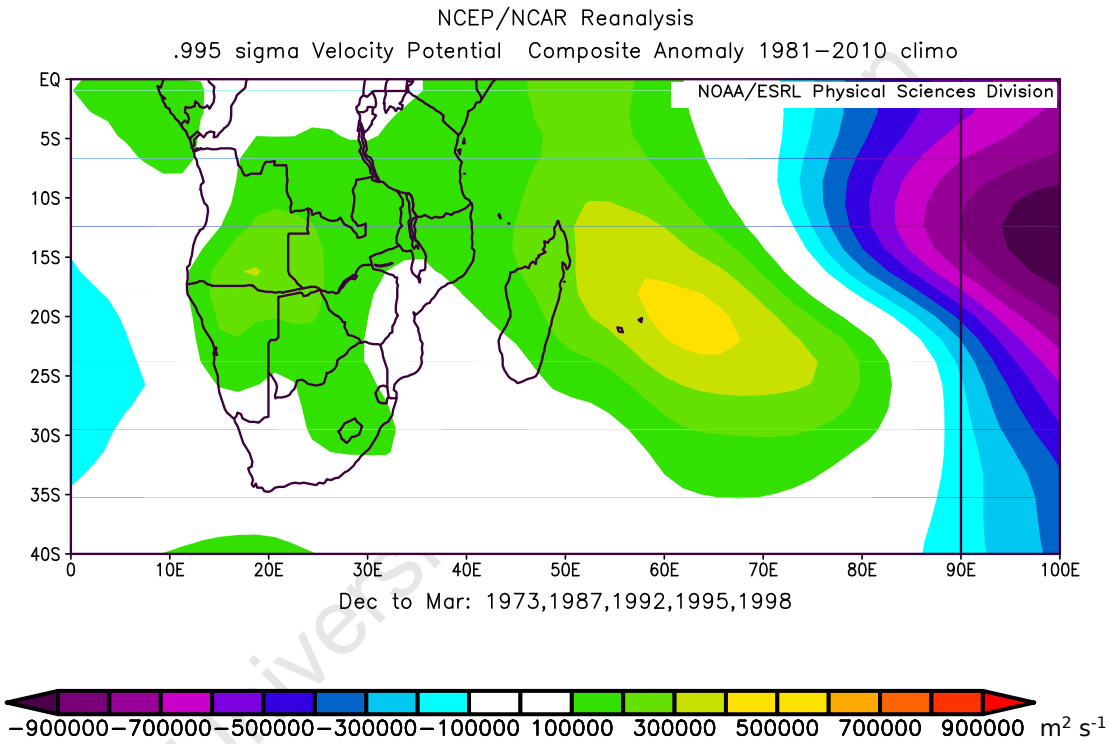

Figure 4.16: Composite anomaly of velocity potential for Dec–Mar of El Niño years (1972–73, 1977–78, 1982–83,1986–87,1991–92,1994–95,1997–98).

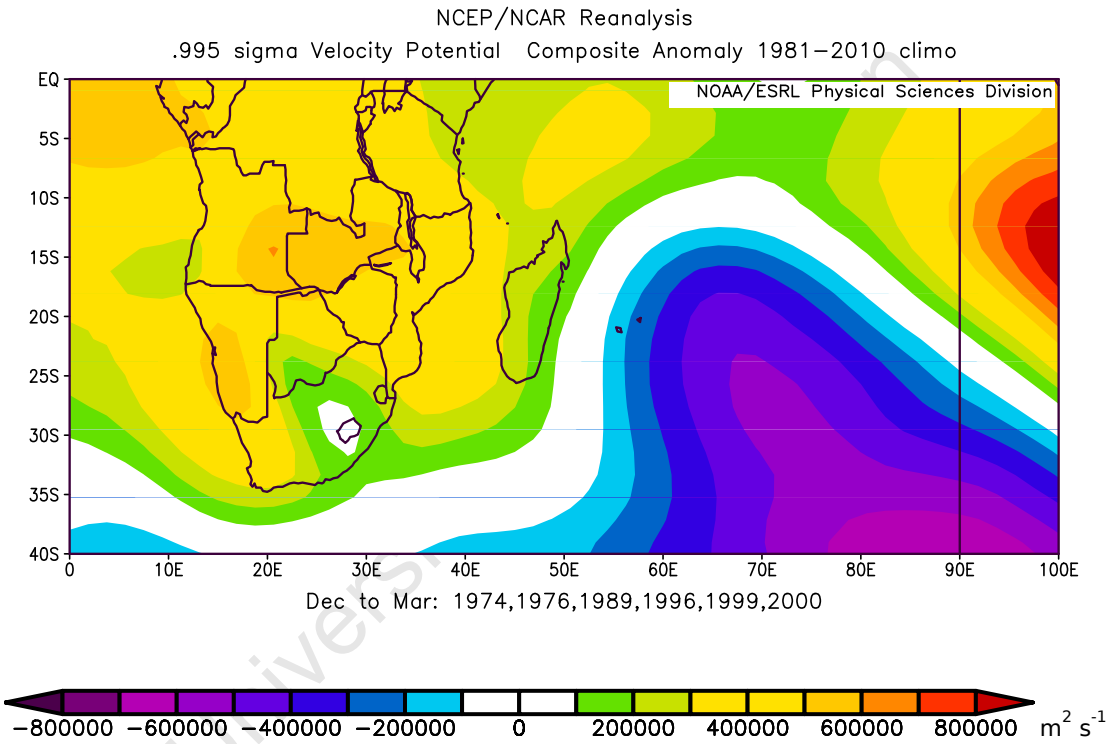

Figure 4.17: Composite anomaly of velocity potential for Dec–Mar velocity potential of La Niña years (1973–74,1975–76,1988–89,1995–96,1998–99,1999–00).

During the summer season December 1979 to March 1980, neutral season having anomalous low frequency of wet days in southwestern Madagascar, a negative anomaly of velocity potential at low level is seen in the entire southern Africa and Madagascar, Figure 4.18. The anomaly is stronger in the south of the Mozambique Channel. While positive anomaly is observed in the Indian Ocean between about 25°S and 15°S. These observations suggest that the ascending branch of the Walker cell shifted eastward to the southern central Indian Ocean during this dry season.

During the El Niño dry year 1991–92, the anomaly of the velocity potential at .995 sigma level shows a strong negative anomaly over southwestern Madagascar and the southern Mozambique Channel, as seen in Figure 4.19. The negative anomaly is weaker over south-eastern Africa. A positive anomaly is observed over the region of the Indian Ocean between about 40°S to 12°S and 65°E to 100°E. These circulation anomalies may suggest an eastward displacement to the southern central Indian Ocean of the ascending branch of Walker cell.

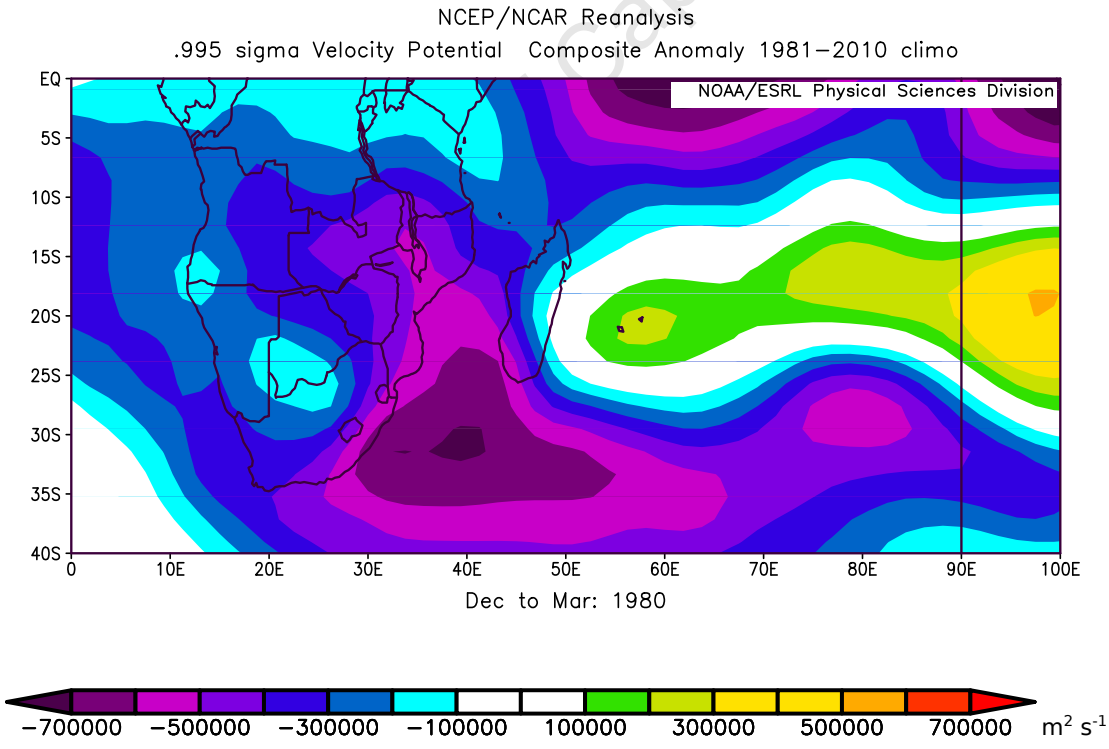

Figure 4.18: Anomalies of velocity potential at .995 sigma level for Dec 1979 –Mar 1980 which is a neutral (non-ENSO) year with low frequency of summer wet days.

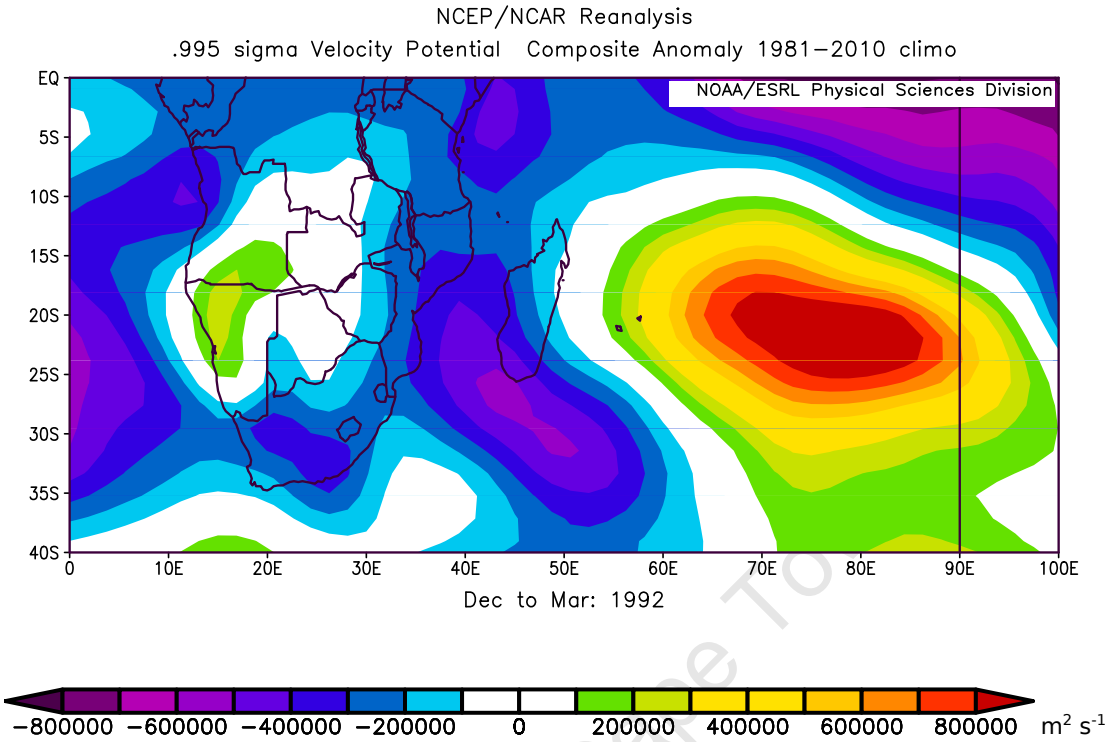

Figure 4.19: Anomalies of velocity potential at .995 sigma level for Dec 1991 –Mar 1992 which is an El Niño year with low frequency of wet days.

The anomaly plot of .995 sigma velocity potential during the neutral wet summer December 1981 to March 1982, Figure 4.20, shows a negative anomaly in southwestern Africa and the southeastern Indian Ocean. The anomaly would suggest a descending limb of the Walker cell over these regions during this season.

In Figure 4.21, positive anomaly of the velocity potential at .995 sigma level is shown in the entire southern Africa and southwestern Madagascar during the wet La Niña season 1998–99. It would suggest that the ascending limb of the Walker cell shifts westward to the African continent, which reinforce the conditions that favour increased frequency of wet days in southwestern Madagascar. In the region of India Ocean between 40°S to 10°S and 50°E to 100°E, a strong descending limb of the Walker cell may result from the strong negative anomaly seen in this region.

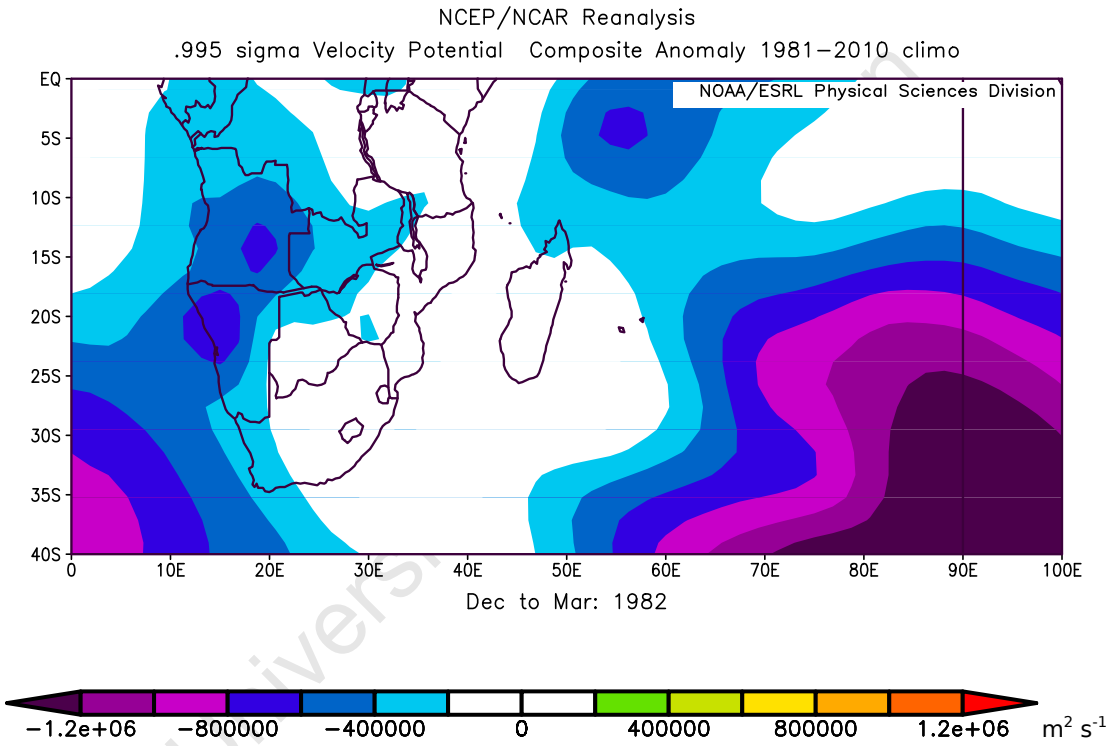

Figure 4.20: Anomalies of velocity potential at .995 sigma level for Dec 1981–Mar 1982 which is a neutral (non-ENSO) season with high frequency of wet days.

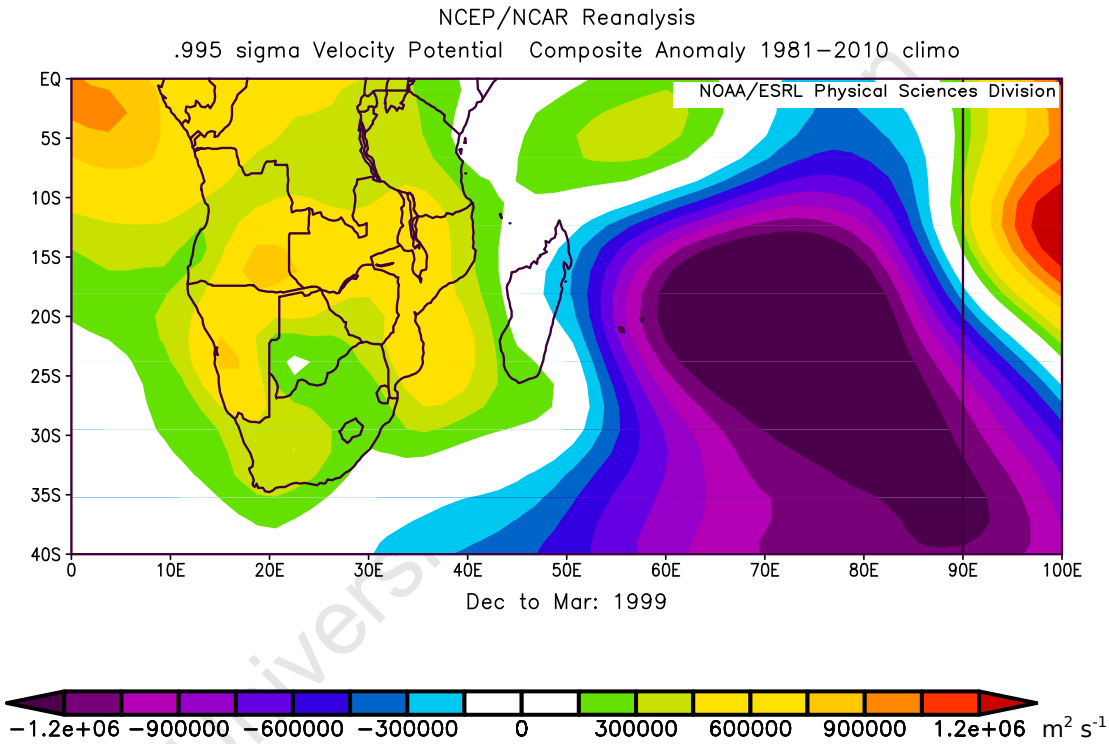

Figure 4.21: Anomalies of velocity potential at .995 sigma level for Dec 1998–Mar 1999 which is a La Niña season with high frequency of wet days.

Chapter 5

Summary and conclusion

Interannual variability of summer rainfall over southwestern Madagascar for the period 1971–2000 was investigated. Rainfall is prominent during summer season (December to March) in Madagascar. The distribution of rainfall is not uniform in the entire island. Significant difference in land elevation over the country, a variety of wind regimes blowing over the country, and tropical cyclones influence its climatic variability. Impacts of topography on wind circulation determines the distribution of rainfall over Madagascar. Southwestern Madagascar receives the least precipitation during the entire year. The annual rainfall amount is between 300 mm and 1000 mm.

Based on the number of wet days (rainfall amount $\geq$1 mm) at the four stations studied (Figure 2.1), the rainy season in southwestern Madagascar starts in December and ends in March, except for Taolagnaro station which has a high frequency of wet days during the entire year (Figure 3.1). The number of wet days during summer, less of than 50% of the total number of days (Figure 3.3), confirms that southwest Madagascar is the driest region of Madagascar (Donque, 1975; Pelleray, 1954). Standardised departures of the frequency of wet days at the four stations show that the driest years are 1979–1980 (neutral year) and 1991–92 (El Niño) for Morondava, Ranohira and Toliara; and the wettest years are 1981–82 (neutral year) and 1998–99 (La Niña) for the four stations (Figure 3.4). Increased (decreased) frequency of wet days might occur with La Niña (El Niño) in southwestern Madagascar.

Direct calculation from the Climate Explorer website showed that the anomaly of the

frequency of wet days over southwestern Madagascar is inversely correlated with the equatorial Pacific SST anomaly. The correlation is the strongest and the most significant for Toliara station ($r < -0.5$ and $p < 0.01$ for Niño1+2, Niño3, Niño3.4 and Niño4). The correlation is weak and less significant for the three other stations (Morondava, Ranohira, Taolagnaro). While direct relationship may exist between frequency of wet days at Toliara and Ranohira and SST in the subtropical southwestern Indian Ocean.

Increased (decreased) the frequency of wet days in summer might be associated with low (high) atmospheric pressure over the south Atlantic Ocean, southern Africa, the southern Mozambique Channel, the Indian Ocean and the western Pacific. A southward displacement of ITCZ during southern hemisphere summer and the presence of reversal of westerly monsoonal wind in the northeast favour conditions of increased frequency of wet days at Morondava, Ranohira and Toliara stations.

Examination of the composite anomalies of the circulations associated with El Niño seasons between 1971 and 2000 concludes: a southerly moisture flux anomaly at 850 hPa associated with weak divergence over Madagascar, a slow descent of air masses at 500 hPa surface pressure over southern Africa and Madagascar, a relative ascent of the branch of the Walker cell in the southwestern Indian Ocean. The composite anomalies of the circulations associated with La Niña seasons between 1971 and 2000 reveals: a northeasterly moisture flux anomaly at 850 hPa associated with weak convergence over Madagascar, a slow ascent of air masses at 500 hPa over Madagascar and a westward displacement of the ascending branch of Walker cell to Madagascar and southern Africa.

Almost similar patterns to the El Niño (La Niña) seasons composite anomalies were found during the driest El Niño season 1991–92 (the wettest La Niña season 1998–99). The differences are the northwesterly moisture flux anomaly over southwestern Madagascar during the La Niña season 1998–99 and an eastward shift of the ascending branch of the Walker cell to the central southern Indian Ocean during the El Niño season 1991–92. The driest neutral season 1979–80 was dominated by a southeasterly moisture flux anomaly over southern Madagascar, a relative descent of air masses over western Madagascar and the Mozambique Channel. An eastward displacement of the ascending branch of the Walker cell might occur. The wettest neutral season 1981–82 is characterised by import of moisture into southern Madagascar, a relative ascent of mass of air at 500 hPa over Madagascar.

In summary, ENSO is one of the dominant modes of interannual variability associated

with summer rainfall over southwestern Madagascar. Despite the significant spatial variation of summer rainfall over southwestern Madagascar, ENSO has an obvious modulating impact on the rainfall over the region. But the influence of SIOD on summer rainfall over southwestern Madagascar cannot be neglected for some regions. Northerly moisture flux anomaly at 850 hPa converging over southwestern Madagascar and occurrence of low atmospheric pressure over the southern Mozambique Channel are favourable conditions for increased number of wet days over southwestern Madagascar. Southerly moisture flux anomaly at 850 hPa over southwestern Madagascar may reduce the number of wet days in the region.

This study focused on interannual variability of the frequency of wet days over southwestern Madagascar and the regional and global circulation patterns that could be associated with the anomaly of the frequency of wet days. Investigation on variability of wet and dry spells over southwestern Madagascar would give another approach of rainfall patterns in the region. The results found in this study could be useful for predicting dry years in southwestern Madagascar which may be needed for food security policies.

Bibliography

Ash, K. D. and Matyas, C. J. (2012). "The influences of ENSO and the subtropical Indian Ocean Dipole on tropical cyclone trajectories in the southwestern Indian Ocean". *International Journal of Climatology* 32.1, pp. 41–56.

Behera, S. K. and Yamagata, T. (2001). "Subtropical SST dipole events in the southern Indian Ocean". *Geophysical Research Letters* 28.2, pp. 327–330.

Donque, G. (1975). *Contribution géographique à l'étude du climat de Madagascar*. Nouv. Impr. des Arts Graphiques, Antananarivo.

Jury, M. R. and Pathack, B. (1991). "A study of climate and weather variability over the tropical southwest Indian Ocean". *Meteorology and Atmospheric Physics* 47 (1), pp. 37–48.

Jury, M. R., Parker, B. A., Raholijao, N., and Nassor, A. (1995). "Variability of summer rainfall over Madagascar: Climatic determinants at interannual scales". *International Journal of Climatology* 15.12, pp. 1323–1332.

Kalnay, E., Kanamitsu, M., Kistler, R., Collins, W., Deaven, D., Gandin, L., Iredell, M., Saha, S., White, G., Woollen, J., et al. (1996). "The NCEP/NCAR 40-year reanalysis project". *Bulletin of the American meteorological Society* 77.3, pp. 437–471.

Nassor, A. and Jury, M. R. (1997). "Intra-seasonal climate variability of Madagascar. Part 2: evolution of flood events". *Meteorology and Atmospheric Physics* 64.3, pp. 243–254.

— (1998). "Intra-seasonal climate variability of Madagascar. Part 1: Mean summer conditions". *Meteorology and Atmospheric Physics* 41, pp. 31–41.

Nicholson, S. E. and Kim, J. (1997). "The relationship of the El Nino-Southern oscillation to African rainfall". *International Journal of Climatology* 17.2, pp. 117–135.

Peixoto, J. P. and Oort, A. H. (1992). *Physics of Climate*. American Institute of Physics.

Pelleray, H. (1954). "Quelques données de base en vue de l'étude des régimes hydrologiques de Madagascar". *Mémoires de l'Institut scientifique de Madagascar* 6.D, pp. 43–86.

Philander, S. G. (1990). *El Niño, La Niña, and the southern oscillation*. Vol. 46. Academic Press.

Poisson, C. (1936). *Documentation statistique sur les cyclones malgaches*. Publications du Service météorologique de Madagascar.

Randriamanga, S., Lahuec, J-P, Dagorne, D., Pennarun, J., and Guillot, B. (1995). "La sécheresse de 1990-1991 et de 1991-1992 à Madagascar vue à partir des images infrarouges Météosat et les données conventionnelles". FRE. In: *Télédétection des ressources en eau : cinquièmes journées scientifiques du réseau Télédétection de l'AUPELF-UREF*, pp. 291–304.

Reason, C. J. C. (2001). "Subtropical Indian Ocean SST dipole events and southern African rainfall". *Geophys. Res. Lett.* 28.11, pp. 2225–2227.

Reason, C. J. C., Allan, R. J., Lindesay, J. A., and Ansell, T. J. (2000). "ENSO and climatic signals across the Indian Ocean basin in the global context: Part I, Interannual composite patterns". *International Journal of Climatology* 20.11, pp. 1285–1327.

Ropelwski, C. F. (1987). "Global and regional scale precipitation patterns associated with the El Niño/ Southern Oscillation." *Monthly Weather Review* 115, pp. 1606–1626.

Sarachik, E. S. and Cane, M. A. (2010). *The El Niño-Southern Oscillation Phenomenon*. Cambridge University Press.

Smith, T.M., Reynolds, R.W., Peterson, T. C., and Lawrimore, J. (2008). "Improvements to NOAA's Historical Merged Land-Ocean Surface Temperature Analysis (1880–2006)". *Journal of Climate* 21, pp. 2283–2296.

Wilks, D. S. (Dec. 2005). *Statistical Methods in the Atmospheric Sciences, Volume 91, Second Edition (International Geophysics)*. 2nd ed. Academic Press.

Williams, J. B. (1990). *Some temporal and regional variations of climate in Madagascar*. Overseas Development Natural Resources Institute.

Xue, Y., Smith, T. M., and Reynolds, R. W. (2003). "Interdecadal changes of 30-yr SST normals during 1871–2000". *Journal of Climate* 16, pp. 1601–1612.